An atomistically-meaningful pseudocontinuum representation for the finite monatomic chain with harmonic nearest-neighbor interactions

M. Charlotte

Université de Toulouse, ISAE-SupAero, Institut Clément ADER (CNRS, UMR 5312), 10 Ave Edouard Belin - BP 54032 - 31 055 TOULOUSE Cedex 4, France

Keywords:
Lattice dynamics
Continuumization
Enhanced elasticity
Non-Newtonian inertia
Local atomistic stress
Dynamic pressure
Percussion loads

A B S T R A C T

An atomistically-meaningful pseudocontinuum representation for the nontrivial lattice dynamics of a finite monatomic chain with linear elastic interactions between nearest neighbor atoms is analytically deduced by mean of a dynamic mechanical analysis extending the memory-dependent pseudocontinuum viewpoint suggested in [M. Charlotte and L. Truskinovsky, *Lattice dynamics from a continuum viewpoint*, J. Mech. Phys. Solids, 60, pages 1508–1544 (2012)]. For a correct description of the lattice dynamics at its interstice length scale, the pseudocontinuum model integrates both the bulk and boundary inertial (heat-vibration) effects of the atomistic medium through specific modifications of the classical elastodynamic Newton's law model: these modifications involve a generalization of the D'Alembert's principle of inertial forces and Neumann-Robin's boundary conditions, without increasing the number of initial and boundary conditions of the generic mechanical evolution problem, unlike all other generalized continuum models proposed in the literature up to this date. Owing to the spatially local and one-dimensional nature of the discrete and pseudocontinuum models, relationships are thus more clearly pinpointed between the elastodynamic normal stress field of that exact generalized continuum representation and the cohesive (or internal) and inertial forces operating at the lattice sites within the bulk of a finite-size monatomic chain and at its boundary.

1. Introduction

It has been already understood for long that, in order to reconcile the particle viewpoint with the continuum one, the solids with discrete/granular microstructures must be described with nonclassical continuum theories involving multiple length and time scales, and that in linear elasticity those ones are in part or essentially embedded into the phonon dispersion relations. Dispersive properties can be obtained in a continuum framework indeed with various enhancing ingredients such as spatial nonlocality (Blanc et al., 2002; Charlotte and Truskinovsky, 2008; Eringen, 1972; Eringen and Eringen, 1976; Eringen and Kim, 1977; Fafalis et al., 2012; Jirásek, 2004; Kroner, 1968; Krumshansl and Wallis, 1965; Kunin, 1982; Mindlin, 1964, 1965; Pichugin et al., 2008; Rogula, 1982; Silling, 2000; Suiker and de Borst, 2005; Sunyk and Steinmann, 2003; Toupin, 1962), temporal nonlocality (Askes et al., 2008; Bishop, 1952; Charlotte and Truskinovsky, 2012; Jirásek, 2004; Love, 2009; Metrikine and Askes, 2002a,b; Mindlin, 1964; Mindlin and Herrmann, 1950; Mindlin and McNiven, 1960; Mühlhaus and Oka, 1996; Pichugin et al., 2008; Rayleigh, 1945) or/and multi-fields/modes (Charlotte and Truskinovsky, 2008; Cosserat and Cosserat, 1909; Eringen, 1966; Eringen and Eringen, 1976; Eringen and Liebowitz, 1968; Il'iushina, 1969; Kunin, 1982; Mindlin and Herrmann, 1950; Mindlin and McNiven, 1960; Vasiliev et al., 2010) while using different kinematic and mechanic arguments. However, some of these enhanced continuum models lack of a physical reality or a mathematical consistency as they do not take into account correctly the dispersive, attenuating, and inertial effects related to the discrete distributions of masses (Charlotte and Truskinovsky, 2012; Milton and Willis, 2007; Willis, 1981; Willis and Suquet, 1997). One can meet for instance some difficulties to ensure the stability of these continuum models with respect to short wavelengths (Charlotte and Truskinovsky, 2008, 2012; Jirásek, 2004; Kunin, 1982; Pichugin et al., 2008; Rogula, 1982; Suiker and de Borst, 2005), or else to predict the filtering of high-frequency phonons that are linked to the natural capabilities of the aforementioned microstructured media to dissipate certain singularities in the material particle motions.

Besides, and apart from the fact that it is not always clear how to consider initial and boundary/interfacial conditions for the prior enhanced continuum models (except by variational formulation when possible), another important difficulty for all these continuum-atomistic connections is to correctly relate quantities

E-mail address: miguel.charlotte@isae.fr

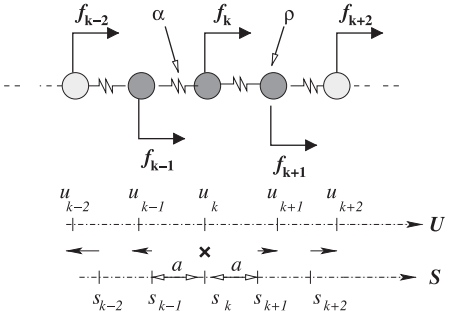

Fig. 1. The generic monatomic chain and its pseudocontinuum reference domain $\mathcal{S}$.

such as strain and stress tensors between two levels, but also these same quantities to forces and displacements used in the molecular model (Zimmerman et al., 2002, 2004, 2010). This may require in particular a correct atomistic interpretation of the local Cauchy's or Piola-Kirchhoff's stress tensors. That last nontrivial point has been a subject of great debate and controversy (see for instance Zhou, 2003). This important issue has been explored from many different perspectives for nearly two hundred years and has led to various definitions that do not appear to be consistent with each other; moreover those ones have not often fully appreciated the difference between pointwise stress measures and temporal and/or spatially-averaged quantities, as reported by Admal and Tadmor (2010, 2016); Murdoch (1982, 2003, 2007); Murdoch and Bedeaux (1993, 1994); Zimmerman et al. (2002, 2004, 2010). Currently, there are at least three definitions for the stress tensor which are commonly used in atomistic simulations: the virial stress (Clausius, 1870; Maxwell, 1870, 1874), the Tsai's traction (Tsai, 1979) and the Hardy's stress (Hardy, 1982). Other coarse grained continuum models use other averaged Cauchy's stress definitions associated with the names of Irving and Kirkwood (1950), Lehoucq and Lilienfeld-Toal (2010); Noll (1955, 2009) (which may be related to the one inferred for the peridynamics (Lehoucq and Silling, 2008; Silling, 2000)), or Murdoch and Bedeaux (Admal and Tadmor, 2010, 2016; Murdoch, 1982, 2003, 2007; Murdoch and Bedeaux, 1993, 1994), to mention just a few them; those ones are in a general multi-dimensional Eulerian's description of granular materials with arbitrary pair potentials of interactions or central cohesive forces between particles.

At the margins of these different viewpoints, this work attempts to identify what kind of local atomistic stress concept can be associated with an accurate *temporally nonlocal pseudocontinuum*[1] (**TN PC**) representation of a finite chain of particles with nearest neighbor harmonic interactions (**NNI**) like the one depicted on Fig. 1, that is submitted to soft loading devices and where the *surface dynamic pressure* generated by the particle vibration at the chain boundary needs to be accounted for as well. The elastodynamics of this Born-Von Kármán's finite, one-dimensional, monoatomic lattice corresponds to the simplest *medium of simple structure*, according to Kunin's classification (Kunin, 1982), since the only kinematic variable is a displacement (vector) that determines the state of the medium completely. However, from the continuum viewpoint, the fine dynamic behavior of such a simple lattice is in fact very complex already even in its linear regime due to the intrinsic occurrence of multiple scales of length and times of evolution (Brillouin and Parodi, 1956; Charlotte and Truskinovsky, 2008, 2012; Kunin, 1982; Maradudin et al., 1971) (as hereinafter the two time-scales ω_*^{-1} and T^* and two length-scales a and L) and to the importance of the micro-structural inertial forces.

The aforementioned TN PC viewpoint that is on target here is the one introduced previously in Charlotte and Truskinovsky (2012) for an infinite lattice domain: it assumes that the non-trivial dynamics of the considered lattice model can be interpreted within that continuous framework by the presence of inertial and pseudo-dissipative post-Newtonian forces yielding a spatio-temporal blending of the inertial and elastic forces. Compared to Charlotte and Truskinovsky (2012) and the many numerical or analytical works that have dealt with the considered lattice model, this new analytical development shows two main novelties: firstly, the inertial forces of the lattice model induce an *elastodynamic normal stress field* satisfying *nonstandard Neumann-Robin's boundary conditions*, with notably *time-dependent properties* in the TN PC model; secondly, the elastodynamic normal stress field of TN PC model can be related to a *simple atomistic interpretation* at the atom level. With this pseudocontinuum modeling, the dispersion of elementary wave-functions (or phonons) generated by the singular loading pulses becomes possible and prohibits the propagation of singularities in $\mathcal{S}$ characterizing the well-known failure of the classical continuum (**CC**) theory under impact load or sudden unloading. Thus, by its salient features of memory-dependent/hereditary media (that have also been anticipated for other dispersive vibrational properties of lattices and periodic material systems such as metamaterials (Milton and Willis, 2007; Willis, 1981; Willis and Suquet, 1997) for instance), the TN PC contrast with the spatially nonlocal pseudocontinuum (**SN PC**) model proposed by Eringen (1972); Eringen and Eringen (1976); Eringen and Kim (1977), Krumshansl and Wallis (1965), Kunin (1982), Rogula (1982). Indeed that latter assumes clearly distinguishable classical inertia and a strong spatial nonlocal elasticity yielding in fact a spatial blending of the bulk and boundary forces (as will demonstrate a subsequent article on this finite chain and boundary loading effects). Additionally, by not placing any restriction on the support of the applied loading in order to deal with point impact loadings as naturally as the original discrete theory, the TN PC model manages to overcome one major drawback of the derived SN PC model, which can be both applicable and accurate only for certain types of data that make the SN model inoperable and unenforceable with concentrated loads.

This paper is organized as follows. As standard in continuum mechanics, the formulation of the TN PC model relies on a specific space-time description of the particle system displacements. Section 2 begins therefore by reminding the main properties of the discrete chain motion and how the particle displacements $\boldsymbol{u}$ can be analytically expressed in terms of the one of the two "natural" continuous interpolation fields G of the discrete impulse response of this mechanical model. To illustrate some specifities of the particle displacements $\boldsymbol{u}$, a couple of complementary tests are purposely performed, one is taken from a singular category and the other one is taken from a smooth category. Section 3 presents then the memory/history dependent continuum mechanics that can be derived from the molecular foundation to include the scale dependence of mass density and boundaries of solid bodies. The main steps of the derivation of that TN model are first discussed, based on the properties of the continuous kernel G. This yields integrodifferential equations of motion involving a generalized linear momentum field $I_1[u]$, generalized normal stress field $I_\varepsilon[u]$ and the additional inertial forces $I_p^{\text{surf}}[u]$ acting at the boundary. It is shown

[1] In *nonlocal elasticity* theories, the notion of *pseudo-continuum, i.e.*continuum theories incorporating internal space and time scales, was also called *quasi-continuum* in the sense of Krumshansl and Wallis (1965), Kunin (1982) and Rogula (1982) (see also Eringen, 1982). Historically, this concept was introduced to treat discrete and continuous elastic models in the scope of the same formalism (Kunin, 1982), what fortuitously may help multi-scale numerical methods coupling (generalized) continuous model with atomistic-lattice ones. Following partly the original idea of Kunin, the term *quasicontinuum* was later purposely borrowed and introduced in the computational mechanics by Shenoy et al. (1999); Tadmor et al. (1996) as a multi-scale numerical method coupling the *classical continuum elasticity* theory with the *nonlocal atomistic-crystal lattice* one. Developing such an averaging computational viewpoint is not however the purpose of this article.

then that an equivalence with the generic discrete model is recoverable from the prediction of this TN model with singular representations of the external and initial inertial loads. In particular, for that TN PC theory, the interpolating displacement field u is merely the response to concentrated loading conditions. Section 4 shows then that the related continuum stress field $I_\varepsilon[u]$ is linked to a specific interpretation of the discrete atomistic forces. Connections with few other derivations in the litterature are also briefly discussed. Finally, some perspectives of investigation are outlined in the concluding Section 5.

2. The discrete linear elastodynamic model

2.1. Material description and loads

Material properties. The lattice dynamics model considered in this work is a basic finite chain of $(N+1)$-ordered particles, with $N \geq 2$, as the one shown in Fig. 1, the particles being labeled with integers $k \in \mathcal{N} \overset{\text{def}}{=} \{0, 1, \ldots, N\}$. The (lattice) parameter $a > 0$ denotes the reference lattice length scale of the considered chain model and $L \overset{\text{def}}{=} Na$ its reference total length. Then the mass of a single particle is defined as ρa, where $\rho > 0$ represents the lineic mass density with respect to a reference continuum $\mathcal{S} \subseteq a\mathbb{R}$ overlapping the reference lattice $a\mathcal{N}$. Each particle interacts only with its nearest neighbors through weightless linear elastic springs with elasticity constant αa where $\alpha > 0$ is the elastic modulus of that chain. Usually, the material constants allow to coarsely assess the reference time

$$\omega_*^{-1} \overset{\text{def}}{=} \frac{a}{2}\sqrt{\frac{\rho}{\alpha}} = \frac{a}{2c} \tag{1}$$

and the propagating wave speed limit $c \overset{\text{def}}{=} \sqrt{\alpha/\rho}$ that are specific from the macroscopic viewpoint of the classical continuumization based on the long wavelength deformations.

Kinematic hypotheses of motion and load conditions. The kinematic and load fields involved in the considered discrete linear mechanical problem are best described in the framework of generalized function (distribution) theory for causal evolutions (Roddier, 1971; Schwartz, 1966; Schwartz, 1983); while broadening the class of admissible loading inputs that can be applied onto the chain, this framework allows to derive and highlight the appropriate class of admissible continuous systems linked to the TN PC model. To deal with the allowed singularities, the (*particle* or *material*) partial time derivative of a (scalar or vector-valued) function $y(t)$ in the usual/classical sense of continuous functions, denoted as $\dot{y}(t)$, will be explicitly distinguished when necessary from the one in the Schwartz' causal distribution sense $D_t y(t)$. As seen hereafter for both the discrete mechanical model and the TN PC one, the allowed kinematic singularities occur in fact only under the action of singular external loading corresponding to impacts.

Regarding more specifically the atomic chain kinematics, here the particles are only allowed to move colinearly (either longitudinally or transversally) to the chain, their time-dependent displacements $\boldsymbol{u}(t) = \{u_k(t)\}_{k\in\mathcal{N}}$ being measured so from the homogeneous lattice equilibrium position. These displacements $\boldsymbol{u}(t)$ are assumed to be continuous (as verified a posteriori, even with localized impact loadings) while excluding however particle collisions for simplicity[2], each of particle velocities $\dot{\boldsymbol{u}}(t) = \{\dot{u}_k(t)\}_{k\in\mathcal{N}}$ may possibly be discontinuous. Moreover, the following initial values are notably ascribed to the displacements and velocities

$$\big(\boldsymbol{u}(0), \dot{\boldsymbol{u}}(0^-)\big) = \big(\boldsymbol{u}^o, \boldsymbol{v}^o\big) \quad \text{with} \quad \boldsymbol{u}^o \overset{\text{def}}{=} \{u_k^o\}_{k\in\mathcal{N}} \quad \text{and} \quad \boldsymbol{v}^o \overset{\text{def}}{=} \{v_k^o\}_{k\in\mathcal{N}}. \tag{2}$$

The departure from the last configurational state is partly generated by applied external forces $a\boldsymbol{f}(t) = \{af_k(t)\}_{k\in\mathcal{N}}$. These ones are assumed to be time-varying generalized functions giving $\boldsymbol{f}(t) \equiv 0$ for $t < 0$ and possessing appropriated properties of growth and singularity in time for $t > 0$. For instance, as shown hereafter each loading contribution af_k will be allowed to impact at a non-accumulating point set of instants like

$$\mathcal{T}_{\mathrm{I}}[f_k](t) \overset{\text{def}}{=} \Big\{t_q \in [0,t];\ \text{ s.c. } \bar{p}_k(t_q) \neq 0\Big\}_{q\in\mathbb{N}}, \ \text{ for } t \in \omega_*^{-1}\mathbb{R}, \tag{3}$$

in a way that af_k can be decomposed into a sum of a piecewise continuous time varying function $a\tilde{f}_k(t)$ and a set of impulses of impact $\{\bar{p}_k(t_p)\}_{t_p\in\mathcal{T}_{\mathrm{I}}[f_k](t)}$, like

$$af_k(t) = a\tilde{f}_k(t) + \sum_{t_p\in\mathcal{T}_{\mathrm{I}}[f_k](t)} \bar{p}_k(t_p)\,\delta_+(t-t_p). \tag{4}$$

These impact load formulas involve the "causal" Dirac's delta function

$$\delta_+(t) \equiv D_t \mathrm{H}(t) \overset{\text{def}}{=} \lim_{\epsilon\searrow 0^+} \frac{\mathrm{H}(t) - \mathrm{H}(t-\epsilon)}{\epsilon}, \tag{5}$$

which represents the generalized partial time derivative of the Heaviside's step function

$$\mathrm{H}(t) \overset{\text{def}}{=} \begin{cases} 0, & \text{if } t < 0 \\ 1, & \text{if } t \geq 0 \end{cases}. \tag{6}$$

For the generalized external loads $a\boldsymbol{f}(t)$ in (4), one can measure then both its impulses with

$$a\int_0^t f_k(\hat{t})\,d\hat{t} = a\int_0^t \tilde{f}_k(\hat{t})\,d\hat{t} + \sum_{t_p\in\mathcal{T}_{\mathrm{I}}[f_k](t)} \bar{p}_k(t_p)\,\mathrm{H}(t-t_p) \ \text{ for } (k,t) \in \mathcal{N}\times\omega_*^{-1}\mathbb{R} \tag{7}$$

and the work done within the motion displacements $\boldsymbol{u}$ by a classical regularizing limit process like

$$\mathcal{P}_g[\boldsymbol{f},\boldsymbol{u}](t) \overset{\text{def}}{=} \lim_{\epsilon\searrow 0} \mathcal{P}_r[\boldsymbol{f}^\epsilon,\boldsymbol{u}^\epsilon](t) \equiv \lim_{\epsilon\searrow 0} \int_0^t \sum_{k\in\mathcal{N}} af_k^\epsilon(\check{t})\,\dot{u}_k^\epsilon(\check{t})\,d\check{t} \tag{8}$$

where

$$\lim_{\epsilon\searrow 0}(\boldsymbol{f}^\epsilon(t), \boldsymbol{u}^\epsilon(t)) = (\boldsymbol{f}(t), \boldsymbol{u}(t)), \ \text{ with } \boldsymbol{f}^\epsilon(t) \equiv 0 \text{ for } t \leq 0. \tag{9}$$

In that regularizing limit process, $\mathcal{P}_g[\boldsymbol{f},\boldsymbol{u}](t)$ can be interpreted as a generalized function of t while $\mathcal{P}_r[\boldsymbol{f},\boldsymbol{u}](t)$ as a standard (regular) function of t; $\boldsymbol{f}^\epsilon(t) = \{f_k^\epsilon(t)\}_{k\in\mathcal{N}}$ represents any sequence of non-impacting (or sufficiently regular time-varying) load functions that (like for instance the one that is implicitly proposed at Eq. (5)) distributionally tends toward the generic loads $\boldsymbol{f}(t)$ formed by the components in Eq. (4); lately, $\boldsymbol{u}^\epsilon(t) = \{u_k^\epsilon(t)\}_{k\in\mathcal{N}}$ represents the sequence of displacement functions outputed by the forthcoming Newtonian equations with $\boldsymbol{f}^\epsilon(t)$ and that distributionally tends to $\boldsymbol{u}(t)$.

2.2. The chain dynamic motion

The Newtonian equations of motion. Within the framework of Schwartz' generalized function (distribution) theory (Roddier, 1971; Schwartz, 1966, 1983), the $(N-1)$-bulk equations and its two Neumann's boundary equations[3] that govern the dynamical motion of

[2] This hypothesis allows so to mimic crystal solid properties but it may be released if the aim is to model granular crystals with contact interactions.

[3] Dirichlet's boundary conditions can also be considered but they would not lead information about the surface inertial forces that are of interest in this analysis.

this chain of $(N+1)$ particles from its initial configuration state given by Eq. (2) can be described in two equivalent forms. Denoting the Kronecker's symbol as $\delta_{k,\,p}$ for any couple of integers $(k,\,p)\in\mathbb{Z}^2$, the more classical form is constituted by

$$\rho D_t^2 u_k = \frac{\alpha}{a^2}\Big\{\big[u_{k+1}-u_k\big](1-\delta_{k,N})+\big[u_{k-1}-u_k\big](1-\delta_{k,0})\Big\} + f_k,\ \text{for}\ (k,t)\in\mathcal{N}\times\omega_*^{-1}\mathbb{R}^+ \tag{10}$$

and must be completed by the initial conditions in (2). Like in Charlotte and Truskinovsky (2012), the equivalent causal form is less classical and involves only

$$\rho D_t^2[\mathrm{H}u_k] = \frac{\alpha}{a^2}\mathrm{H}\Big\{\big[u_{k+1}-u_k\big](1-\delta_{k,N})+\big[u_{k-1}-u_k\big](1-\delta_{k,0})\Big\} + f_k+\rho\mathcal{D}_t^2 u_k,\ \text{for}\ (k,t)\in\mathcal{N}\times\omega_*^{-1}\mathbb{R} \tag{11a}$$

the following *initial inertial loads* replacing the initial conditions in (2)

$$\rho a\mathfrak{D}_t^2\boldsymbol{u}(t) = \big\{\rho a\mathfrak{D}_t^2 u_k(t)\big\}_{k\in\mathcal{N}} \overset{\text{def}}{=} \rho a\big[\boldsymbol{v}^o\,\delta_+(t)+\boldsymbol{u}^o\,D_t\delta_+(t)\big],\quad \text{for}\, t\in\omega_*^{-1}\mathbb{R}. \tag{11b}$$

This causal formulation of the dynamic motions has certain advantages. It notably allows a clear analysis of the balance of forces in action and of their effects. In particular, by summing the set of Eqs. (11a), one can infer accordingly with the principle of conservation of momentum that no overall dynamic rigid motion of translation can occur for the chain barycenter if the external loading and initial kinematic data satisfy

$$a\sum_{k\in\mathcal{N}}\big[f_k(t)+\rho\mathfrak{D}_t^2 u_k(t)\big]=0,\ \text{for}\ t\in\omega_*^{-1}\mathbb{R}. \tag{12}$$

For convenience, the following analysis will consider only such a type of loading cases.

Lately, a meaningful expression of work for the initial inertial loads $\rho a\mathfrak{D}_t^2\boldsymbol{u}(t)$ can moreover be associated like

$$\mathcal{P}_{\text{init}}[\rho\mathfrak{D}_t^2\boldsymbol{u},\boldsymbol{u}](t)\overset{\text{def}}{=}\mathrm{H}(t)\,\rho a\sum_{k\in\mathcal{N}}\Big[v_k^o\,\dot{u}_k(0^+)-u_k^o\ddot{u}_k(0^+)\Big]. \tag{13}$$

The latter can be interpreted with respect to the ones in Eq. (8) as follows if $\boldsymbol{f}(0^+)=\boldsymbol{0}$[4] (and no particle collision) at initial time

$$\mathcal{P}_{\text{init}}[\rho\mathfrak{D}_t^2\boldsymbol{u},\boldsymbol{u}](t)\equiv\mathcal{P}_g[\rho\mathfrak{D}_t^2\boldsymbol{u},\boldsymbol{u}](t)\equiv\mathcal{P}_r[\rho\mathfrak{D}_t^2\boldsymbol{u},\boldsymbol{u}](t) \equiv 2\mathcal{E}_{\mathrm{e}}[\boldsymbol{u}](0)+2\mathcal{E}_{\mathrm{k}}[\boldsymbol{u}](0). \tag{14}$$

The last equivalence in Eq. (14) follows by virtue of the Euler's theorem for homogeneous functions and the initial expression of the classical Newtonian equations of motion for $\boldsymbol{u}(t)$ in (10) at $t=0^+$ (and therefore $D_t^2u_k(0^+)=\ddot{u}_k(0^+)$). It introduces the initial value of the Hamiltonian potential energy of classical mechanics, with the elastic potential energy

$$\mathcal{E}_{\mathrm{e}}[\boldsymbol{u}](t)\overset{\text{def}}{=}a\sum_{k=1}^{N}\frac{\alpha}{2}\left[\frac{u_k(t)-u_{k-1}(t)}{a}\right]^2,\ \text{for}\ t\in\omega_*^{-1}\mathbb{R}^+ \tag{15a}$$

and the kinetic energy

$$\mathcal{E}_{\mathrm{k}}[\boldsymbol{u}](t)\overset{\text{def}}{=}a\sum_{k=0}^{N}\frac{\rho}{2}\Big[\dot{u}_k(t)\Big]^2,\ \text{for almost all}\ t\in\omega_*^{-1}\mathbb{R}^+ \tag{15b}$$

that are well-defined only at instants $t\geq 0$ where the couple $(\boldsymbol{u}(t),\,D_t\boldsymbol{u}(t))$ is regular.

[4] Otherwise, in presence of external load impacts, this kind of Clapeyron's theorem of "potential energy" equivalence (Love, 1927) can be applied only to the "homogeneous" (or complementary) part of the solution $\boldsymbol{u}$ that depends only on the initial kinematical conditions.

Solution of motion. The solution of the Cauchy's initial boundary value problem (**IBVP**) formulated in (11) can be analytically obtained by using the **(LT)** Laplace Transform, which is couched in this analysis for any arbitrary function of time $y(t)$ like

$$y(t)\overset{\mathbf{LT}}{\to}y(\omega)=\int_0^\infty y(t)\,\mathrm{e}^{-i\omega t}dt,\ \text{for}\ \Im m(\omega)<-\check{\omega}_b\leq 0; \tag{16a}$$

accordingly, its inversion is obtained with the following formulas

$$y(\omega)\to y(t)=\frac{1}{2\pi}\int_{-i\omega_b-\infty}^{-i\omega_b+\infty}y(\omega)\,\mathrm{e}^{i\omega t}d\omega.\forall\omega_b>\check{\omega}_b\geq 0. \tag{16b}$$

The positive real number $\check{\omega}_b$ in (16a) must notably be sufficiently large to ensure the existence of the integral as a holomorphic function over a semi-plane of the complex plane $\omega_*\mathbb{C}$; $\Re e(\cdot)$ and $\Im m(\cdot)$ denote respectively the real and imaginary parts of the complex number in argument; i is the principal square-root determination of the imaginary number related to $i^2=-1$.

The LT of the Cauchy's IBVP in (10) and (2) and the one in (11a), lead to the same auxiliary spectral boundary value problem (**BVP**), which is

$$-\rho\,\omega^2u_k(\omega)=\frac{\alpha}{a^2}\Big\{\big[u_{k+1}(\omega)-u_k(\omega)\big](1-\delta_{k,N}) + \big[u_{k-1}(\omega)-u_k(\omega)\big](1-\delta_{k,0})\Big\}\ +\ f_k(\omega)\ +\ \mathfrak{D}_t^2u_k(\omega) \tag{17}$$

for $k\in\mathcal{N}$ and where $\mathfrak{D}_t^2\boldsymbol{u}(\omega)=i\omega\boldsymbol{u}^o+\boldsymbol{v}^o$. The solution of the BVP in (17) can be obtained analytically in Laplace space by the well-known Green function method that provides formally

$$u_k(\omega)=\sum_{j\in\mathcal{N}}G(ka,ja,\omega)\Big[\frac{f_j(\omega)}{\rho}+\mathfrak{D}_t^2u_j(\omega)\Big],\ \text{for}\ k\in\mathcal{N}. \tag{18}$$

We look then for the kernel $G(s,\hat{s},\omega)$ for $(s,\hat{s})\in([0,L])^2$ that solves the BVP constituted by the bulk equations for $(k,\,p)\in(\mathcal{N}\setminus\{0,N\})^2$

$$\rho\,\omega^2G(ka,pa,\omega)+\frac{\alpha}{a^2}[G(ka+a,pa,\omega)+G(ka-a,pa,\omega) -2G(ka,pa,\omega)]=-\rho\,\delta_{k,p} \tag{19a}$$

and the boundary conditions for $p\in\mathcal{N}$ (and while reminding $L=Na$)

$$-\rho\,\omega^2G(0,pa,\omega)=\frac{\alpha}{a^2}\big[G(a,pa,\omega)-G(0,pa,\omega)\big]+\rho\,\delta_{0,p}, \tag{19b}$$

$$-\rho\,\omega^2G(L,pa,\omega)=\frac{\alpha}{a^2}\big[G(L-a,pa,\omega)-G(L,pa,\omega)\big]+\rho\,\delta_{N,p}. \tag{19c}$$

One can also replace these *inhomogeneous* Robin-like boundary conditions by the following *homogeneous* Neumann-like ones

$$\alpha\big[G(0,\hat{s},\omega)-G(-a,\hat{s},\omega)\big]=0\ \text{ and }\ \alpha\big[G(L+a,\hat{s},\omega)-G(L,\hat{s},\omega)\big]=0,\ \text{for}\ \hat{s}\in[0,L]. \tag{20}$$

It follows that one can explicitly couch

$$G(s,\hat{s},\omega)\overset{\text{def}}{=}-\frac{\rho a^2}{2\alpha} \times\frac{\cos\big(\lambda_o(\omega)(L-|s-\hat{s}|+a)\big)+\cos\big(\lambda_o(\omega)(L-s-\hat{s})\big)}{\sin\big(\lambda_o(\omega)a\big)\sin\big(\lambda_o(\omega)(L+a)\big)},\quad \text{for}\ (s,\hat{s})\in([0,L])^2. \tag{21}$$

This last one can also be continuously extended to all $(s,\hat{s})\in(a\mathbb{R})^2$). It conveys several important information to spectrally characterize the time-dependent material properties of the considered lattice model amongst which the following complex function

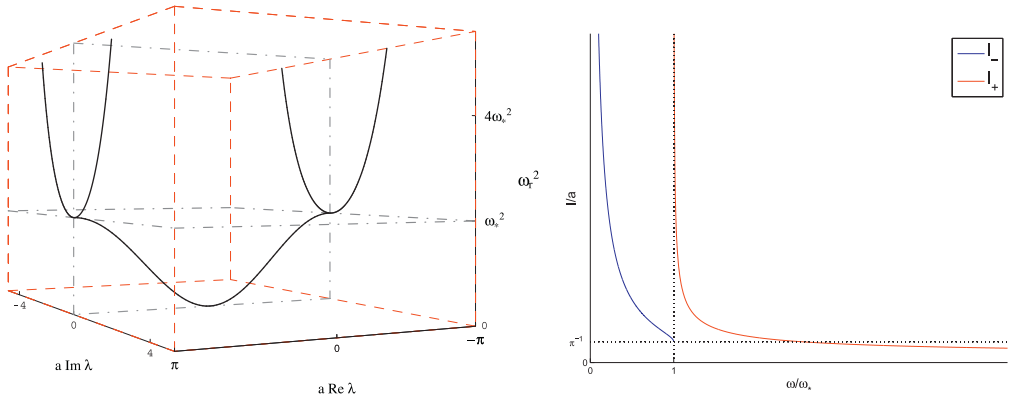

(a) (b)

Fig. 2. Phonon dispersion and attenuation curves $(\lambda_o(\omega), \omega^2) \in a^{-1}\mathbb{C} \times \omega_*^2\mathbb{R}^+$ with in (a) the dispersion relation $\lambda = \lambda_o(\omega)$ with $\omega = \omega_r + i0^{\pm}$ (see (Charlotte and Truskinovsky, 2012) for evolution details) and in (b) the phonon propagation wavelength $\ell_-(\omega_r)$ and the phonon attenuation wavelength $\ell_+(\omega_r)$; these lengths are respectively defined from that the lower and upper branches of the dispersion curves $\lambda_o(\omega)$ in a.

$$\lambda_o(\omega) \stackrel{\text{def}}{=} \frac{-i}{a}\,\log\left(1-\frac{2\omega^2}{\omega_*^2}-2i\frac{\omega}{\omega_*}\sqrt{1-\frac{\omega^2}{\omega_*^2}}\right) \equiv -\frac{2}{a}\arcsin\left(\frac{\omega}{\omega_*}\right) \tag{22}$$

that is well-defined everywhere in $\omega_*\mathbb{C}$ outside the branch-cuts $\mathcal{C} \stackrel{\text{def}}{=} \omega_*\mathbb{R} \setminus [-\omega_*, \omega_*]$.

From the viewpoint of an infinite chain case with finite $a = L/N$ (*viz.*the thermodynamic limit), $\lambda_o(\omega)$ for $\omega \in \omega_*\mathbb{R}$ defines an explicit dispersion-relation, which is illustrated on Fig. 2(a). Its full image is located into the strip

$$\mathbb{B}_0 \stackrel{\text{def}}{=} \left\{\lambda = \lambda_r + i\lambda_i \in a^{-1}\mathbb{C};\ |\lambda_r a| \le \pi\,,\ (\lambda_r a, \lambda_i a) \in \mathbb{R}^2\right\} \tag{23}$$

that contains the fundamental Brillouin's interval $\mathbb{K} \stackrel{\text{def}}{=} \big[-\pi/a, \pi/a\big]$. Following (Brillouin and Parodi, 1956; Charlotte and Truskinovsky, 2012), one can define then from $\lambda_o(\omega)$ for $\omega \in \omega_*\mathbb{R}$ two important frequency-dependent wavelengths:
one is for the propagation of waves (or phonons) through the chain, as well as their observable interferences into resonant standing modes (also said stationary or normal modes) of vibration at specific frequencies $\{\omega_p\}_{p\in\mathcal{N}}$ (given in Appendix A),

$$\ell_-(\omega) \stackrel{\text{def}}{=} \frac{a}{\arccos\left(1-\frac{2\omega^2}{\omega_*^2}\right)} \equiv |\lambda_o(\omega)|^{-1} \in [0, \pi\,],$$
$$\text{for } \omega \in [-\omega_*, \omega_*], \tag{24a}$$

the other one is for their attenuation through chain by (local) inertia,

$$\ell_+(\omega) \stackrel{\text{def}}{=} \frac{a}{\ln\left[\frac{2\omega^2}{\omega_*^2}-1+\frac{2|\omega|}{\omega_*}\sqrt{\frac{\omega^2}{\omega_*^2}-1}\right]} \equiv \left|\lambda_o(\omega)+\frac{\pi}{a}\mathrm{sgn}(\omega)\right|^{-1}$$
$$\ge 0, \ \text{ for } \omega \in \mathcal{C}. \tag{24b}$$

Moreover, the following functions (while reminding (1)) represent respectively, for $\omega \in [-\omega_*, \omega_*]$, the group and phase velocities of propagating waves that are relevant for physicists and acoustic engineers

$$c_{\text{gr}}(\omega) \stackrel{\text{def}}{=} -\frac{d\omega}{d\lambda_o}(\lambda_o(\omega)) \equiv \frac{\omega_* a}{2}\cos(\lambda_o(\omega)a/2) \equiv c\sqrt{1-\frac{\omega^2}{\omega_*^2}} \tag{25a}$$

$$c_{\text{ph}}(\omega) \stackrel{\text{def}}{=} -\frac{\omega}{\lambda_o(\omega)} \equiv \frac{\omega_*\sin(\lambda_o(\omega)a/2)}{\lambda_o(\omega)} \equiv c\frac{\sin(\lambda_o(\omega)a/2)}{\lambda_o(\omega)a/2}. \tag{25b}$$

Now in time space, the solution of the Cauchy's problem in (10) and (2), as well as in (11a), is like

$$u_k(t) = \sum_{j\in\mathcal{N}}\Big[\int_0^t G(ka, ja, t-\hat{t})\frac{f_j(\hat{t})}{\rho}d\hat{t} + D_t\widehat{G}(ka, ja, t)u_j^o + \widehat{G}(ka, ja, t)v_j^o\Big],$$
$$\text{for } (k,t) \in \mathcal{N}\times\omega_*^{-1}\mathbb{R}. \tag{26}$$

The last expression for $u_k(t)$ relies on the following acausal kernel (that can also be extended for $(s,\hat{s}) \in (a\mathbb{R})^2$)

$$\widehat{G}(s,\hat{s},t) \stackrel{\text{def}}{=} G(s,\hat{s},t) - G(s,\hat{s},-t) \equiv \mathrm{sgn}(t)\,G(s,\hat{s},|t|),$$
$$\text{for } (s,\hat{s},t) \in (a\mathcal{N})^2\times\omega_*^{-1}\mathbb{R}, \tag{27}$$

which is defined from the causal kernel

$$G(s,\hat{s},t) \equiv \mathrm{H}(t)\,\widehat{G}(s,\hat{s},t) = \frac{1}{2\pi}\int_{-i\omega_b-\infty}^{-i\omega_b+\infty} G(s,\hat{s},\omega)\,\mathrm{e}^{i\omega t}\,d\omega,$$
$$\text{for} (s,\hat{s},t) \in (a\mathcal{N})^2\times\omega_*^{-1}\mathbb{R}. \tag{28}$$

The latter that is computed explicitly in Appendix A and its LT $G(s,\hat{s},\omega)$ in (21) satisfy important difference-differential properties that are worth mentioning for the comparison with the integro-differential ones in Appendix B. Notably, $G(s,\hat{s},t)$ solves the IBVP formed by the following system of equations for $(k,p,t) \in \mathcal{N}^2\times\omega_*^{-1}\mathbb{R}$

$$\rho\,D_t^2G(ka,pa,t) = \frac{\alpha}{a^2}\Big\{\Big[G(ka+a,pa,t)-G(ka,pa,t)\Big](1-\delta_{k,N}) + \Big[G(ka-a,pa,t)-G(ka,pa,t)\Big](1-\delta_{k,0})\Big\} + \rho\,\delta_{k,p}\,\delta_+(t) \tag{29a}$$

and the initial conditions

$$G(ka,pa,t) \equiv 0, \ \text{ for } (k,p) \in \mathcal{N}^2 \text{ and } t \le 0 \tag{29ba}$$

$$D_tG(ka,pa,0^+) \equiv \dot{G}(ka,pa,0^+) = \delta_{k,p}, \ \text{ for } (k,p) \in \mathcal{N}^2. \tag{29bb}$$

2.3. Quasiperiodic and nonlocal features of the atomistic motions

The dynamic motion of this lattice has nontrivial features that are not so well-known and deserve therefore a special emphasis. Some of these features can be illustrated with the two following types of standard rheological tests.

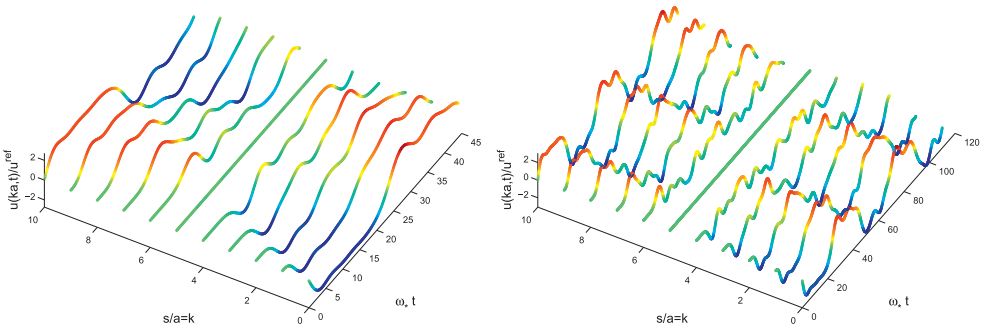

(a) $t \in [0, T^*]$ (b) $t \in [0, 5T^*/2]$

Fig. 3. Impact test responses with $N = L/a = 10$: the normalized displacements $\boldsymbol{u}(t)/u^{\text{ref}}$ (with $u^{\text{ref}} = \bar{p}/\rho\omega_* a = \bar{p}/2\rho c$) of the $(N+1)$-atoms over two intervals of time. The time T^* represents the pseudo-period of vibration of the chain introduced in Eq. (35) and the displacements $\boldsymbol{u}(t)$ are analytically given by Eq. (31).

Impact tests. Here a simple self-balanced couple of impact loads (or equivalently, initial velocities) at two points and satisfying (12) is considered. The knowledge of the response of the system to singular impact loading is of fundamental importance in both experimental and theoretical characterization of linear discrete systems because it allows one to fully identify the corresponding Green's functions (which are also named as impulse responses). Moreover such a load is one for which the CC elasto-dynamics fails, as shown in Charlotte and Truskinovsky (2012) for the infinite material domain. Fig. (3) illustrates over different ranges of time the displacement ratios $2\rho c\boldsymbol{u}(t)/\bar{p}$ that are generated by loads $a\boldsymbol{f}(t) = \{af_k(t)\}_{k\in\mathcal{N}}$ impacting the chain with

$$af_k(t) = \bar{p}\,[\delta_{k,N} - \delta_{k,0}]\,\delta_+(t), \tag{30}$$

$\bar{p}$ being a constant real parameter prescribing an impulse at initial time $t = 0$; the chain is initially at its rest state (*i.e.*with $\boldsymbol{u}^o = \boldsymbol{0} = \boldsymbol{v}^o$). According to (26), the resulting displacements $\boldsymbol{u}(t)$ read component-wisely then as follows

$$u_k(t) = [G(ka, L, t) - G(ka, 0, t)]\frac{\bar{p}}{\rho a}, \text{ for } (k, t) \in \mathcal{N} \times \omega_*^{-1}\mathbb{R}^+. \tag{31}$$

As shown in Appendix C with the more general impacting load cases $\boldsymbol{f}$ in (4), the energy introduced in the system can be computed analytically with the expression of work in (8) and accordingly with Eqs. (29b), giving so

$$\mathcal{P}_g[\boldsymbol{f}, \boldsymbol{u}](t) = \mathrm{H}(t)\sum_{k\in\mathcal{N}} \bar{p}_k(0)\,\dot{u}_k(0^+) = 2\mathrm{H}(t)\,\frac{\bar{p}^2}{\rho a} \equiv \mathcal{P}_r[\boldsymbol{f}, \boldsymbol{u}](t), \quad \text{for } t \in \omega_*^{-1}\mathbb{R}. \tag{32}$$

Release test. Here a release test from initial displacements is chosen to identify some complementary time-dependent properties which cannot fully be identified with the impulse responses of the impact test. To observe these other relevant temporal properties, one can consider the responses due to the simple initial displacements $\boldsymbol{u}^o = \{u_k^o\}_{k\in\mathcal{N}}$ where

$$u_k^o = \bar{u}\,[\delta_{k,N} - \delta_{k,0}] \tag{33}$$

while the constant real parameter $\bar{u}$ prescribes the initial displacements at initial time $t = 0$; besides the following initial velocity $\boldsymbol{v}^o = \boldsymbol{0}$ and external load $\boldsymbol{f}(t) = \boldsymbol{0}$ are imposed. Fig. (4) illustrates the resulting free displacement ratios $\boldsymbol{u}(t)/\bar{u}$ of the chain particles, which component-wisely read like

$$u_k(t) = \bar{u}\,D_t[\widehat{G}(ka, L, t) - \widehat{G}(ka, 0, t)]. \tag{34}$$

Following (Charlotte and Truskinovsky, 2012), the expression of instantaneous work in (13) combined with Eq. (29) attribute the following initial energy to the system

$$\mathcal{P}_{\text{init}}[\rho\mathfrak{D}_t^2\boldsymbol{u}, \boldsymbol{u}](t) = -\mathrm{H}(t)\,\rho a\sum_{k\in\mathcal{N}} u_k^o\ddot{u}_k(0^+) = 2\mathrm{H}(t)\,\frac{\rho c^2\bar{u}^2}{a}, \text{ for } t \in \omega_*^{-1}\mathbb{R}.$$

The salient features exhibited by the two previous rheological tests deserve further comments. Indeed, a specific consequence of the wave dispersion and attenuation is that the free oscillations of this chain of $(N+1)$ material points in Figs. 3 and 4 are generally not exactly periodic in time, but exhibit small fluctuations. As already mentioned by Lagrange (1853) (see also Myshkis and Filimonov, 2003), this arises because the angular frequencies $\{\omega_p\}_{p\in\mathcal{N}}$ of the eigenmodes of vibration $\{(\omega_p, \{\mathcal{F}_p(ka)\}_{k\in\mathcal{N}})\}_{p\in\mathcal{N}}$ of the system (that are specified in Appendix A) are pairwise incommensurable; in fact, an exact periodicity can occur only if both the initial and loading conditions are constituted by one same and unique monochromatic (one-wavelength) basis function $\mathcal{F}_p(s)$ of deformation. Nevertheless, the (free) vibrational displacements $\boldsymbol{u}(t)$ like those generated by the previous tests are almost periodic and have their pseudo-period

$$T^* \stackrel{\text{def}}{=} 2(L + a)/c \equiv 4(N + 1)/\omega_*. \tag{35}$$

The small aperiodic fluctuations produce intriguing microstructural overshoot effects (that may possibly be important notably for the safety of the structure if preliminarily extended near to certain critical values) for sudden unloadings (Petrov et al., 2008), as for impacts (Charlotte and Truskinovsky, 2012; Slepyan, 1972).

Another specific (but hardly noticeable) feature that is caused by the massless elastic interaction between the particles is that this strain-able finite discrete model reacts instantaneously in a nontrivial pseudo-rigid fashion that differs from both the classical rigid solid and the classical continuum bar model (Charlotte and Truskinovsky, 2012; Wolf, 1979). This statement can be substantiated here again by considering nonzero initial data and the impact loading only at one single given atom $p \in \mathcal{N}$, like for instance

$$u_k(0) = u_k^o = \bar{u}\delta_{k,p},\ \dot{u}_k(0^-) = v_k^o = \bar{v}\delta_{k,p},\ a\,f_k(t) = \bar{p}\,\delta_+(t)\,\delta_{k,p} \quad \text{for } k \in \mathcal{N}$$

where again $(\bar{u}, \bar{v}, \bar{p})$ are constant parameters. The general solution (26) can be written so as

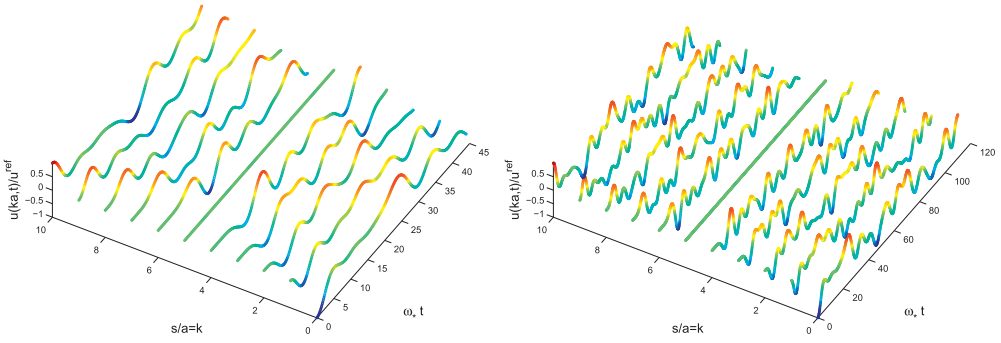

(a) $t \in [0, T^*]$ (b) $t \in [0, 5T^*/2]$

Fig. 4. Release test responses with $N = L/a = 10$: the normalized displacements $\boldsymbol{u}(t)/u^{\text{ref}}$ (with $u^{\text{ref}} = \bar{u}$) of the $(N+1)$-atoms over two intervals of time. The displacements $\boldsymbol{u}(t)$ are analytically given by Eq. (34).

$$u_k(t) = \bar{u}\, D_t \widehat{G}(ka, pa, t) + \left(\frac{\bar{p}}{\rho a}\, \mathrm{H}(t) + \bar{v}\right) \widehat{G}(ka, pa, t)$$
$$\text{for } (k,t) \in \mathcal{N} \times \omega_*^{-1}\mathbb{R}$$

and, by using notably (11) and (29), provides then

$$\dot{u}_k(0^+) = \left(\frac{\bar{p}}{\rho a} + \bar{v}\right) \delta_{k,p},\ \ddot{u}_k(0^+)$$
$$= \frac{\omega_*^2}{4}\bar{u}\big\{\big[\delta_{k+1,p} - \delta_{k,p}\big](1-\delta_{k,N})$$
$$+ \big[\delta_{k-1,p} - \delta_{k,p}\big](1-\delta_{k,0})\big\},\ \text{etc.}$$

One can infer then that the higher the order of the time-derivative of the non-rigid deformation vector $\{u_k(t) - u_p(t)\}_{k\in\mathcal{N}}$ at $t = 0^+$, the larger is the number of particles affected by these perturbations. This nontrivial nonlocal feature expresses the fact that the concept of a sharp deformation front or a finite deformation cone, which is common in continuum models, can be viewed only as a coarse approximation.

3. The temporally nonlocal pseudocontinuum model

Let us develop now the TN PC model that is capable of capturing the thermal vibration effects that are observed at the microscopic time and space scales $|\omega^{-1}| \sim \omega_*^{-1}$ and $|\lambda^{-1}| \sim a$. The adaptation of the TN viewpoint developed in Charlotte and Truskinovsky (2012) to the case of a bounded domain loaded by soft loading devices requires to identify some natural boundary conditions, which are the purpose of this section and one of the two new main results of this communication. As the model is here *spatially local*, what is notably expressed by the fact that the dispersion curves of the discrete and TN PC models are given only by a unique function $\lambda_o(\omega)$, bulk and boundary contributions are initially distinguished as for the (local) CC theory.

3.1. Derivation of the model

Formally, the TN PC model of interest can be related to a Cauchy's IBVP involving a bounded continuum domain like $\mathcal{S} = [0, L]$ and a bulk equation like

$$I_1[u](s,t) - D_s I_\varepsilon[u](s,t) = f(s,t) + \rho \mathfrak{D}_t^2 u(s,t),$$
$$\text{for } (s,t) \in]0, L[\times\omega_*^{-1}\mathbb{R}. \tag{36a}$$

The functionals $I_1[u](s,t)$, $D_s I_\varepsilon[u](s,t)$ and $I_\varepsilon[u](s,t)$ represent respectively the linear momentum forces, the bulk linear elastic forces and the bulk (normal) stress linked to the displacement fields $u(s,t)$ of the TN PC model. The main argument of the current contribution is that, for the proposed TN model, the *natural* boundary conditions at the extremities $s \in \{0, L\}$ of the domain $\mathcal{S} = [0, L]$ can be a priori found as specific generalized Neumann-Robin's impedance boundary conditions

$$I_p^{\text{surf}}[u](0,t) - I_\varepsilon[u](0^+,t) = a f_0(t) + \rho a \mathfrak{D}_t^2 u_0(t); \tag{36b}$$

$$I_p^{\text{surf}}[u](L,t) + I_\varepsilon[u](L^-,t) = a f_N(t) + \rho a \mathfrak{D}_t^2 u_N(t). \tag{36c}$$

Here, an additional functional $-I_p^{\text{surf}}[u](s,t)$ representing "internal" generalized inertial forces acting at the continuum domain boundary with $(s,t) \in \{0,L\} \times \omega_*^{-1}(\mathbb{R}^+ \setminus \{0\})$ must also be identified. Besides, again as in Charlotte and Truskinovsky (2012) the load density $f(s,t)$ and the following initial inertial force density (per unit of length)

$$\rho \mathfrak{D}_t^2 u(s,t) \overset{\text{def}}{=} \rho\Big[v^o(s)\,\delta_+(t) + u^o(s)\,D_t\delta_+(t)\Big] \tag{37}$$

are related to their discrete analogous sequences $\boldsymbol{f}(t)$ and $\rho\mathfrak{D}_t^2\boldsymbol{u}(t)$ through the general formulas of interpolation

$$u^o(s) \overset{\text{def}}{=} \sum_{k\in\mathcal{N}} \kappa_{k,0}(s/a)\, u_k^o,\ \ v^o(s) \overset{\text{def}}{=} \sum_{k\in\mathcal{N}} \kappa_{k,1}(s/a)\, v_k^o \text{ and } f(s,t)$$
$$\overset{\text{def}}{=} \sum_{k\in\mathcal{N}} \kappa_{k,2}(s/a)\, f_k(t). \tag{38}$$

A particular interest will be for the case where the interpolation kernels $\{\kappa_{k,p}\}_{(k,p)\in\mathcal{N}\times\{0,1,2\}}$ for these external loads and pre-inertial ones are proportional to the spatial Dirac's delta function

$$\delta(s) \overset{\text{def}}{=} D_s^2 \frac{|s|}{2} \equiv D_s \frac{\text{sgn}(s)}{2}, \tag{39}$$

while denoting D_s the spatial differential operator in the sense of Schwartz' distribution theory and sgn$(\cdot)$ the signum function.

The appropriate expressions for $I_1[\,\cdot\,](s,t)$, $I_\varepsilon[\,\cdot\,](s,t)$ and $I_p^{\text{surf}}[\cdot](s,t)$ come from analyzing the IBVP solved by the interpolating kernel $G(s,\hat{s},t)$ in (28), but now from the distribution theory of continuous media. This dynamical mechanical analysis is performed in Appendix B. By including some computational details from Charlotte and Truskinovsky (2012), this provides the ensuing bulk integro-differential field operators for $(s,t) \in (\mathcal{S}\setminus\{0,L\}) \times \omega_*^{-1}\mathbb{R}$

$$I_1[u](s,t) \overset{\text{def}}{=} \left[1 + \frac{1}{\omega_*^2} D_t^2\right] \int_0^t u(s,t-\hat{t}) D_{\hat{t}}^3 \Upsilon_1(\hat{t})\ d\hat{t} \tag{40a}$$

$$I_\varepsilon[u](s,t) \overset{\text{def}}{=} \left[1 + \frac{1}{\omega_*^2} D_t^2\right] \int_0^t D_s u(s,t-\hat{t})\, D_{\hat{t}} \Upsilon_2(\hat{t})\, d\hat{t}, \tag{40b}$$

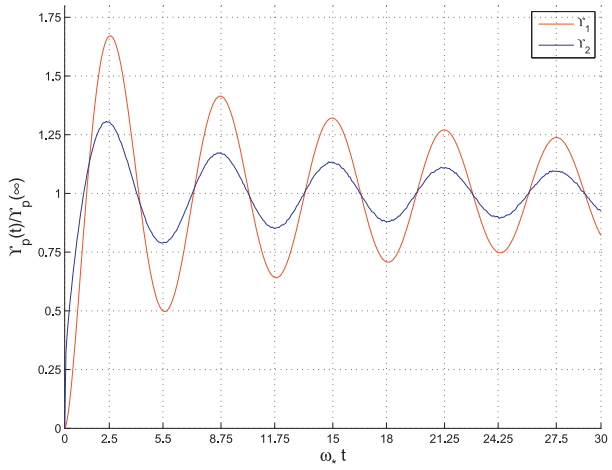

Fig. 5. The mass and elastic density kernels Υ_p $(p = 1, 2)$. Their synchronous transient behaviors start with $\Upsilon_1(t) = 0,\ \Upsilon_2(t) = 0,\ D_t\Upsilon_1(t) = 0,\ D_t^2\Upsilon_1(t) = 0$ for $t \leq 0$; then they approach the long-time asymptotes (for times such as $\omega_* t \gg 1$) $\Upsilon_1(+\infty) = \rho$ and $\Upsilon_2(+\infty) = \alpha$. The deviations $\Upsilon_p(t) - \Upsilon_p(+\infty)$ from these static equilibrium values induce "pseudo-forces of dissipation".

and, for comparison, the ensuing surface integro-differential field one

$$I_p^{\mathrm{surf}}[u](s,t) \overset{\mathrm{def}}{=} a\int_0^t D_t^2\big[\mathrm{H}(t-\hat{t})u(s,t-\hat{t})\big]\,D_{\hat{t}}\Upsilon^{\mathrm{surf}}(\hat{t})\,d\hat{t},$$
$$\text{for } (s,t)\in\{0,L\}\times\omega_*^{-1}\mathbb{R}. \tag{40c}$$

It raises that the linear momentum force functional $I_1[u](s,\,t)$ and (normal) stress functional $I_\varepsilon[u](s,\,t)$ of the PC model are exactly those described in Charlotte and Truskinovsky (2012); they are built with the following time varying functions representing respectively a nontrivial mass density and a nontrivial elastic modulus

$$\Upsilon_1(t) \overset{\mathrm{def}}{=} \mathrm{H}(t)\,\rho\left\{1-\int_{\omega_*}^{\infty}\frac{\omega_*\cos(\omega_r t)}{\omega_r^2\sqrt{\frac{\omega_r^2}{\omega_*^2}-1}}\,d\omega_r\right\}, \tag{41a}$$

$$\Upsilon_2(t) \overset{\mathrm{def}}{=} \mathrm{H}(t)\,\alpha\left\{1-\int_{\omega_*}^{\infty}\frac{4\cos(\omega_r t)\,d\omega_r}{\omega_*\left[\frac{a^2}{\ell_+^2}+\pi^2\right]\sqrt{\frac{\omega_r^2}{\omega_*^2}-1}}\right\}, \tag{41b}$$

which are depicted again on Fig. 5 for convenience. One noteworthy point is that these nontrivial kernels tend towards the classical coarse-scale equilibrium estimates,

$$(\Upsilon_1(+\infty),\,\Upsilon_2(+\infty)) = (\rho,\,\alpha),$$

with vanishing fluctuations $\{\Upsilon_p(t) - \Upsilon_p(+\infty)\}_{p=1,2}$ that are related to the structurally attenuated wave high-frequencies. However, the LT of $\mathrm{Y}_1(t)$ and $\mathrm{Y}_2(t)$ have simple expressions that can also be formulated in terms of the phase and group velocities introduced in Eq. (25) like

$$\Upsilon_1(\omega) = \frac{\rho\lambda_o a}{i\omega\,\sin(\lambda_o a)} = \frac{\rho c^2}{i\omega c_{\mathrm{ph}}(\omega)\,c_{\mathrm{gr}}(\omega)} \quad \text{and}$$
$$\Upsilon_2(\omega) = \frac{4\alpha\omega}{i\omega_*^2\lambda_o a\,\sin(\lambda_o a)} = \frac{\alpha\,c_{\mathrm{ph}}(\omega)}{i\omega\,c_{\mathrm{gr}}(\omega)},$$

where notably $\omega \equiv -\omega_*\sin\big(\lambda_o(\omega)a/2\big)$ and $\alpha \equiv \rho c^2$. It is worth emphasizing similarly that the LTs of the nontrivial linear momentum force and stress functionals also read like

$$I_1[u](s,\omega) = \rho\,\omega_*^2\lambda_o a\,\frac{\sin(\lambda_o a)}{4\omega^2}\,(i\omega)^2 u(s,\omega)$$
$$\equiv \frac{c_{\mathrm{gr}}(\omega)}{c_{\mathrm{ph}}(\omega)}\,\rho\,(i\omega)^2 u(s,\omega) \tag{42}$$

and

$$I_\varepsilon[u](s,\omega) = \frac{\sin(\lambda_o a)}{\lambda_o a}\,\alpha\,D_s u(s,\omega) \equiv \frac{c_{\mathrm{ph}}(\omega)\,c_{\mathrm{gr}}(\omega)}{c^2}\,\alpha D_s u(s,\omega),$$
$$\text{for } s\in\mathcal{S}\setminus\{0,L\}. \tag{43}$$

Besides, the new contribution for this TN model is the following time-varying *apparent mass density* as a kernel for the functional $I_p^{\mathrm{surf}}[u](s,t)$ representing the inertial forces of surface

$$\Upsilon^{\mathrm{surf}}(t) \overset{\mathrm{def}}{=} \frac{\rho}{2}\,\mathrm{H}(t) \quad \text{with } \Upsilon^{\mathrm{surf}}(\omega) = \frac{\rho a}{2i\omega}. \tag{44}$$

As a result, the surface functional in (40c) can merely be read as the following distribution

$$I_p^{\mathrm{surf}}[u](s,t) = \frac{\rho a}{2}\,D_t^2\big[\mathrm{H}(t)u(s,t)\big],\ \text{for } (s,t)\in\{0,L\}\times\omega_*^{-1}\mathbb{R} \tag{45}$$

and its LT can be obtained by replacing G by u in Eq. (B.2c).

Interestingly, these results and those of the forthcoming Section 4 (see Eq. (65)) tend to emphasize the following kind of *surface inertial pressures* (or again *generalized surface mechanical impedance* contributions from the first and last, half-mass, particles of this chain if we adopt Brillouin and Parodi's viewpoint (Brillouin and Parodi, 1956, chap. 5, sec. 22, page 86))

$$\mathfrak{q}(0,t) \overset{\mathrm{def}}{=} I_p^{\mathrm{surf}}[u](0,t) - \frac{\rho a}{2}\mathfrak{D}_t^2 u_0(t) \equiv I_\varepsilon[u](0^-,t) - \frac{\rho a}{2}\mathfrak{D}_t^2 u_0(t); \tag{46a}$$

$$-\mathfrak{q}(L,t) \overset{\mathrm{def}}{=} I_p^{\mathrm{surf}}[u](L,t) - \frac{\rho a}{2}\mathfrak{D}_t^2 u_N(t) \equiv -I_\varepsilon[u](L^+,t)$$
$$-\frac{\rho a}{2}\mathfrak{D}_t^2 u_N(t), \tag{46b}$$

which also read as follows when the velocities at $s \in \{0,\,L\}$ are initially continuous

$$\mathfrak{q}(0,t) \equiv \frac{\rho a}{2}\,\mathrm{H}(t)\,D_t^2 u(0,t) \equiv \frac{\rho a}{2}\,\mathrm{H}(t)\,D_t^2 u_0(t)$$
$$-\mathfrak{q}(L,t) \equiv \frac{\rho a}{2}\,\mathrm{H}(t)\,D_t^2 u(L,t) \equiv \frac{\rho a}{2}\,\mathrm{H}(t)\,D_t^2 u_N(t).$$

The Neumann-Robin's equations in (36b) and (36c) involve such surface inertial pressures like

$$\mathfrak{q}(0,t) - I_\varepsilon[u](0^+,t) - \frac{\rho a}{2}\mathfrak{D}_t^2 u_0(t) = a f_0(t),\ \text{for } t\in\omega_*^{-1}\mathbb{R}; \tag{47a}$$

$$-\mathfrak{q}(L,t) + I_\varepsilon[u](L^-,t) - \frac{\rho a}{2}\mathfrak{D}_t^2 u_N(t) = a f_N(t),\ \text{for } t\in\omega_*^{-1}\mathbb{R}. \tag{47b}$$

As one last relevant feature of this TN PC model, one can also mention how the "fluctuations" of the material constants $\mathrm{Y}_p(t)$ about their observable values $\mathrm{Y}_p(\infty)$ can also be exploited to exhibit the "pseudo-forces of dissipation" embedded within the nontrivial inertial force $I_1[u](s,\,t)$ and the stress $I_\varepsilon[u](s,\,t)$ in Eq. (40), since according to the convolution algebra of the causal distributions

$$I_1[u](s,t) \equiv I_1^e[\hat{u}_0](s,t) + D_t\int_0^t\big[\Upsilon_1(t-\hat{t})-\rho\big]\,D_{\hat{t}}^2\big[\mathrm{H}(\hat{t})\hat{u}_0(s,\hat{t})\big]\,d\hat{t} \tag{48a}$$

$$I_\varepsilon[u](s,t) \equiv I_\varepsilon^e[\hat{u}_0](s,t) + D_s\int_0^t\big[\Upsilon_2(t-\hat{t})-\alpha\big]\,D_{\hat{t}}\big[\mathrm{H}(\hat{t})\hat{u}_0(s,\hat{t})\big]\,d\hat{t}. \tag{48b}$$

These reformulations involve contributions of different intuitive natures. Indeed, there arises on one hand the following conservative (non-dissipative) force and stress

$$I_1^c[\hat{u}_0](s,t) \overset{\text{def}}{=} \rho D_t^2\big[\mathrm{H}(t)\hat{u}_0(s,t)\big];\ \ I_\varepsilon^c[\hat{u}_0](s,t) \overset{\text{def}}{=} \alpha D_s\big[\mathrm{H}(t)\hat{u}_0(s,t)\big],$$
$$\text{for } (s,t) \in \mathcal{S}\times\omega_*^{-1}\mathbb{R} \tag{49}$$

with respect to the displacement field

$$\hat{u}_0(s,t) \overset{\text{def}}{=} \Big[1+\frac{1}{\omega_*^2}D_t^2\Big]u(s,t) \text{ for } (s,t)\in\mathcal{S}\times\omega_*^{-1}\mathbb{R}^+, \tag{50a}$$

which, with the initial conditions

$$\hat{u}_0(s,0)\equiv u(s,0) \text{ and } \dot{\hat{u}}_0(s,0^-)\equiv\dot{\hat{u}}(s,0^-) \text{ for } s\in\mathcal{S}, \tag{50b}$$

provide conversely

$$u(s,t) \equiv \cos(\omega_* t)\hat{u}_0(s,0)+\frac{\sin(\omega_* t)}{\omega_*}\dot{\hat{u}}_0(s,0^-) + \mathrm{H}(t)\int_0^t \frac{\sin(\omega_*(t-\hat{t}))}{\omega_*}\hat{u}_0(s,\hat{t})\,d\hat{t}. \tag{50c}$$

On the other hand, the integral terms in Eq. (48) provide non-conservative (or dissipative) contributions that are associated with the mass and stiffness deviations $\{\Upsilon_p(t)-\Upsilon_p(+\infty)\}_{p=1,2}$ resulting from the structural attenuation (evanescence) of the wave high-frequencies. Obviously, in terms of the new field $\hat{u}_0(s,t)$ that allows a more standard formulation of the momentum and stress relations with generalized constitutive laws[5] (see Eqs. (146), (147) and (148) in Charlotte and Truskinovsky (2012)), this filtering entails some dissipation of high-frequency vibration energies by 'heat' and 'thermal stress'. Accordingly, while taking into account Eqs. (48) and (49), an energy of dissipation can be "measured" with respect to the field $\hat{u}_0(s,t)$ for sufficiently smooth loads, by the standard variational process multiplying the Eq. (36) by $D_t\hat{u}_0(s,t)$ and integrations on space and time variables to arrive then at an energy conservation/balance law.

Naturally, from a coarse scale viewpoint of observation that lasts over sufficiently long time $t\gg\omega_*^{-1}=\sqrt{\rho/\alpha}\,a/2$ with respect to the reference times ω_*^{-1} (or for slow process, sufficiently large ω_* as described by Coleman (1964a,b)) and sufficiently large number $N=L/a$ of particles, the previous fading memory becomes negligible. The chain model behaves macroscopically then like the well-known D'Alembert's *perfectly elastic rod model* whose the governing equation of motion in Schwartz's causal distribution sense

$$I_1^c[u](s,t)-D_s I_\varepsilon^c[u](s,t)=f(s,t)+\rho\mathfrak{D}_t^2u(s,t)$$

(for sufficiently smooth initial and loading conditions) involves then

$$u(s,t)\sim\hat{u}_0(s,t);\ \ I_1^c[u](s,t)\sim I_1^c[\hat{u}_0](s,t);\ \ I_\varepsilon^c[u](s,t)\sim I_\varepsilon^c[\hat{u}_0](s,t).$$

3.2. Analytical solution of the TN PC model

In order to prove the perfect matching of the TN PC with the generic discrete model at the microscopic time and space scales $|\omega^{-1}|\sim\omega_*^{-1}$ and $|\lambda^{-1}|\sim a$, one can analytically solve the IBVP in (36) with (40) and compare their main features. For this, the IBVP is again first projected into the LT variable space. Consecutively, solving the LT of the elastodynamic operator of the equation model in (36) for $u(s,\omega)$ with the Green function method, provides then

$$u(s,\omega)=\int_{\mathcal{S}\setminus\{0,L\}}G(s,\hat{s},\omega)\Big[\frac{f(\hat{s},\omega)}{\rho}+\mathfrak{D}_t^2u(\hat{s},\omega)\Big]\frac{d\hat{s}}{a} + \sum_{p\in\{0,N\}}G(s,pa,\omega)\Big[\frac{f_p(\omega)}{\rho}+\mathfrak{D}_t^2u(pa,\omega)\Big]. \tag{51}$$

Thus the general solution of the TN problem in (36) reads as follows

$$u(s,t)=\int_{\mathcal{S}\setminus\{0,L\}}\Big[\int_0^t G(s,\hat{s},t-\hat{t})\frac{f(\hat{s},\hat{t})}{\rho}\,d\hat{t} + D_t\widehat{G}(s,\hat{s},t)u^o(\hat{s})+\widehat{G}(s,\hat{s},t)v^o(\hat{s})\Big]\frac{d\hat{s}}{a} \times\sum_{p\in\{0,N\}}\Big[\int_0^t G(s,pa,t-\hat{t})\frac{f_p(\hat{t})}{\rho}\,d\hat{t} + D_t\widehat{G}(s,pa,t)u^o(pa)+\widehat{G}(s,pa,t)v^o(pa)\Big] \tag{52}$$

with the interpolating Green's functions $\widehat{G}(s,\hat{s},t)$ and $G(s,\hat{s},t)$ introduced in (27) and (28).

One can immediately infer then that the dynamic solution $u(s,t)$ in (52) corresponds to the following continuous interpolation of the discrete solution $\boldsymbol{u}(t)=\{u_k(t)\}_{k\in\mathcal{N}}$ in (26), with $u(ka,t)\equiv u_k(t)$ for $k\in\mathcal{N}$,

$$u(s,t)=\sum_{j\in\mathcal{N}}\Big[\int_0^t G(s,ja,t-\hat{t})\frac{f_j(\hat{t})}{\rho}d\hat{t} + D_t\widehat{G}(s,ja,t)u_j^o+\widehat{G}(s,ja,t)v_j^o\Big] \tag{53}$$

if the data are interpolated as in Eq. (38) with the singular weight functions (while taking into account the properties of the spatial Dirac's generalized function $\delta(s)$ in (39)

$$\kappa_{k,q}(\eta)=(1-\delta_{k,0}-\delta_{k,N})\delta(\eta-k), \quad \text{for } (q,k,\eta)\in\{0,1,2\}\times\mathcal{N}\times[0,N]. \tag{54}$$

Actually that choice of weight functions even ensures the following equivalences for the total forces for $t\in\omega_*^{-1}\mathbb{R}$

$$\int_{\mathcal{S}\setminus\{0,L\}}f(s,t)\,ds+a\sum_{p\in\{0,N\}}f_p(t)\equiv a\sum_{k\in\mathcal{N}}f_k(t), \tag{55a}$$

$$\int_{\mathcal{S}\setminus\{0,L\}}\rho\mathfrak{D}_t^2u(s,t)\,ds+a\sum_{p\in\{0,N\}}\rho\mathfrak{D}_t^2u_p(t)\equiv a\sum_{k\in\mathcal{N}}\rho\mathfrak{D}_t^2u_k(t). \tag{55b}$$

Moreover, the following classical continuum expressions of generalized and regular works

$$\mathcal{P}_g^c[f,u](t)\overset{\text{def}}{=}\lim_{\epsilon\searrow0}\mathcal{P}_r^c(f^\epsilon,u^\epsilon,t),\ \text{ for }\lim_{\epsilon\searrow0}(f^\epsilon,u^\epsilon)=(f,u) \tag{56a}$$

$$\mathcal{P}_r^c[f,u](t)\overset{\text{def}}{=}\int_0^t\Big[\int_{\mathcal{S}\setminus\{0,L\}}f(s,\check{t})\,\dot{u}(s,\check{t})\,ds + \sum_{p\in\{0,N\}}a\,f_p(\check{t})\,\dot{u}(pa,\check{t})\Big]d\check{t} \tag{56b}$$

$$\mathcal{P}_{\text{init}}^c[\rho\mathfrak{D}_t^2u,u](t)\overset{\text{def}}{=}\mathrm{H}(t)\,\rho\Big\{\int_{\mathcal{S}\setminus\{0,L\}}\big[v^o(s)\,\dot{u}(s,0^+) - u^o(s)\,\ddot{u}(s,0^+)\big]ds + a\sum_{s\in\{0,L\}}\big[v^o(s)\,\dot{u}(s,0^+)-u^o(s)\,\ddot{u}(s,0^+)\big]\Big\} \tag{56c}$$

[5] It was notably pinpointed in Charlotte and Truskinovsky (2012) for an unbounded monatomic chain and a step loading $f(s,t)$, that the new displacement field $\hat{u}_0(s,t)$ allows to capture the main 'macroscopic' phenomenon, while the original displacement field $u(s,t)$ brings additional lattice scale oscillations generated by the 'memory' kernel in (50c). One may say in other words that the displacement deviation $\hat{u}_0(s,t)-u(s,t)=\omega_*^{-2}D_t^2u(s,t)$ measures some kind of thermal vibration property. That latter one calls for an adequate thermodynamic interpretation – what goes however beyond the author's goal and current understanding – but that may possibly be like the *mean displacement magnitude-temperature* one suggested by Green and Naghdi (1991, 1993).

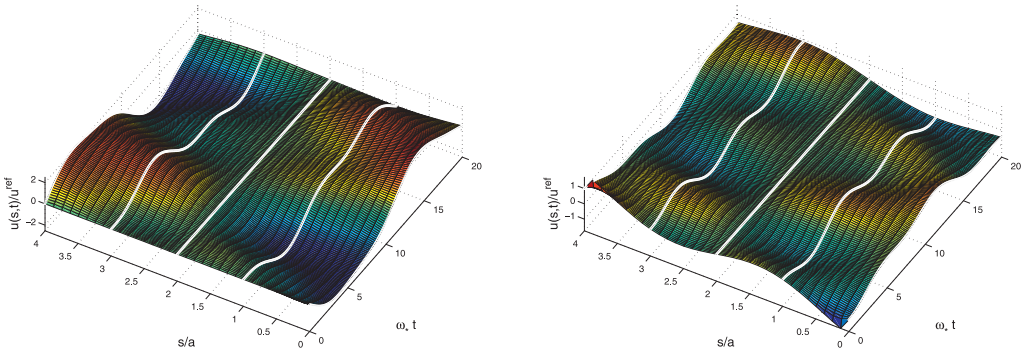

(a) Impact TN with Neumann's b.c. (b) Release TN with Neumann's b.c.

Fig. 6. The normalized responses u/u^{ref} of the TN PC model for $t \in [0, T^*]$ and $N = L/a = 4$, for impact in (b) (*with* $u^{\text{ref}} = \tilde{p}/2\rho c$) *and for initial displacements in* (a) (*with* $u^{\text{ref}} = \tilde{u}$). *The white lines superposed on the TN interpolating field* $u(s, t)$ *represent the displacements* $\boldsymbol{u}(t)$ *of the chain of particles.*

also become equivalent to their discrete counterparts $\mathcal{P}[\boldsymbol{f}, \boldsymbol{u}](t)$ and $\mathcal{P}_{\text{init}}[\rho\mathfrak{D}_t^2\boldsymbol{u}, \boldsymbol{u}](t)$ expressed in (C.9) and (13). Notably, we have $\mathcal{P}_g^c[f, u](t) \equiv \mathcal{P}_r^c[f, u](t)$, while $\mathcal{P}_{\text{init}}^c[\rho\mathfrak{D}_t^2 u, u](t) \equiv \mathcal{P}_r^c[\rho\mathfrak{D}_t^2 u, u](t)$ in absence of impact at the initial time. It is worth mentioning that this perfect interpolating fit for a chain with an arbitrary number of atoms (see Charlotte and Truskinovsky, 2012 for the unbounded case) can also be proven for IBVP cases involving Dirichlet's boundary conditions as well.

Finally, the dynamic motions described by the continuous displacement field $u(s, t)$ in (53) can be illustrated with the same rheologic tests of impact and release used for the discrete model in Section 2.2, what yields for the impact case

$$u(s,t) = [G(s,L,t) - G(s,0,t)]\frac{\tilde{p}}{\rho a} \tag{57}$$

while for the release case

$$u(s,t) = \tilde{u}D_t[\widehat{G}(s,L,t) - \widehat{G}(s,0,t)] \equiv \tilde{u}[\dot{\widehat{G}}(s,L,t) - \dot{\widehat{G}}(s,0,t)]. \tag{58}$$

Fig. 6 shows the displacement field ratio $2\rho cu/\tilde{p}$ (for the impact case) and $u/\tilde{u}$ (for the release case) over the pseudo-period of time T^* of the atomic displacements $\boldsymbol{u}(t)$ that was introduced in (35). The displacements $\boldsymbol{u}(t)$ of the particles are also superposed as white lines on the displacement field $u(s, t)$.

4. Relations between the normal stress and the discrete interaction loads

As already mentioned in the introduction, giving a definition of the local stress in a molecular material is a hot topic in multiscale or hybrid (particle-continuum) modeling where a key issue involves the smooth transfer of information between the discrete model and the continuum one. It is therefore of practical interest to investigate if the stress field $I_\varepsilon[u](s, t)$ in (40b) has a simple *atomistic normal stress* interpretation in terms of the *material internal forces*. This section shows that Newtonian inertial terms (in the sense of D'Alembert) play a relevant role into this interpretation.

Indeed, this interpretation can be obtained by relating the complex stress field $I_\varepsilon[u](s, \omega)$ in (43) to the LT of the interpolating solution field $u(s, t)$ in (53)

$$u(s,\omega) = \sum_{j\in\mathcal{N}}\left[G(s,ja,\omega)\frac{f_j(\omega)}{\rho} + \dot{G}(s,ja,\omega)u_j^o + G(s,ja,\omega)v_j^o\right]. \tag{59}$$

Standard trigonometric relations provide then for any $s \in]0, L[$ and $s_p \overset{\text{def}}{=} pa \in a\mathcal{N}$

$$I_\varepsilon[u](s^-,\omega) - \alpha\frac{u(s,\omega) - u(s-a,\omega)}{a} + \frac{\rho a}{2}\omega^2 u(s,\omega) = \omega_* a\sum_{p=1}^{N-1}\left[f_p(\omega) + \rho\,\mathfrak{D}_t^2 u_p(\omega)\right]i\omega\theta(s_{p+1} - s, \omega);$$

$$I_\varepsilon[u](s^+,\omega) - \alpha\frac{u(s+a,\omega) - u(s,\omega)}{a} - \frac{\rho a}{2}\omega^2 u(s,\omega) = \omega_* a\sum_{p=1}^{N-1}\left[f_p(\omega) + \rho\,\mathfrak{D}_t^2 u_p(\omega)\right]i\omega\theta(s_{p-1} - s, \omega).$$

The foregoing relations involve notably the spectral kernel

$$\theta(s,\omega) \overset{\text{def}}{=} -\mathbb{1}_{[0,a[}(s)\frac{\sin(\lambda_o s)}{i\omega\omega_* \sin(\lambda_o a)} \tag{60}$$

where $\mathbb{1}_\Omega(s)$ denotes the indicator function of the set Ω. The inverse LT of $\theta(s, \omega)$ corresponds to the ensuing weight function with support in $[0, a] \times \omega_*^{-1}\mathbb{R}^+$

$$\theta(s,t) = -\mathbb{1}_{[0,a[}(s)\,\frac{s\,\mathrm{H}(t)}{\omega_* a} \times\left[1 - \operatorname{sinc}\left(\frac{\pi s}{a}\right)\int_{\omega_*}^{\infty}\frac{\omega_*\cosh(\frac{s}{\ell_+})\,\cos(\omega t)}{\omega^2\sqrt{\frac{\omega^2}{\omega_*^2} - 1}}\,d\omega\right] \tag{61a}$$

$$\equiv \mathbb{1}_{[0,a[}(s)\,\frac{\mathrm{H}(t)}{\pi}\left[\cos\left(\frac{\pi s}{a}\right)\int_{\omega_*}^{\infty}\frac{\sinh(\frac{s}{\ell_+})\sin(\omega_r t)}{\omega_r^2\sqrt{\frac{\omega_r^2}{\omega_*^2} - 1}}\,d\omega_r - \int_0^{\omega_*}\frac{\sin(\frac{s}{\ell_-})\sin(\omega_r t)}{\omega_r^2\sqrt{1 - \frac{\omega_r^2}{\omega_*^2}}}\,d\omega_r\right], \tag{61b}$$

notably by virtue of the Cauchy-Goursat's theorem on a closed contour integral paths for $\omega \in \omega_*\mathbb{C}\setminus\mathcal{C}$ with $\Im m(\omega) > 0$, the Jordan's lemma on an infinite upper semicircle with $|\omega/\omega_*| \gg 1$, and the following path integral identity for $s \in [0, a[$ and $t > 0$

$$0 = \int_{i0^+-\infty}^{i0^++\infty} -\theta(s,\lambda)\,\mathrm{e}^{i\omega t}\,d\omega, \text{ for } s \in [0,a[\text{ and } t > 0$$
$$\equiv \int_{\omega_*}^{\infty}\frac{\sin(\pi s/a)\cosh(s/\ell_+)\cos(\omega_r t) - \cos(\pi s/a)\sinh(s/\ell_+)\sin(\omega_r t)}{\omega_r^2\sqrt{\frac{\omega_r^2}{\omega_*^2} - 1}}\,d\omega_r + \int_0^{\omega_*}\frac{\sin(s/\ell_-)\sin(\omega_r t)}{\omega_r^2\sqrt{1 - \frac{\omega_r^2}{\omega_*^2}}}\,d\omega_r - \frac{\pi s}{\omega_* a}.$$

The transient allures of the dimensionless causal function $\omega_*\theta(s, t)$ is depicted on Fig. 7 on its space-time support $[0, a] \times \omega_*^{-1}\mathbb{R}^+$.

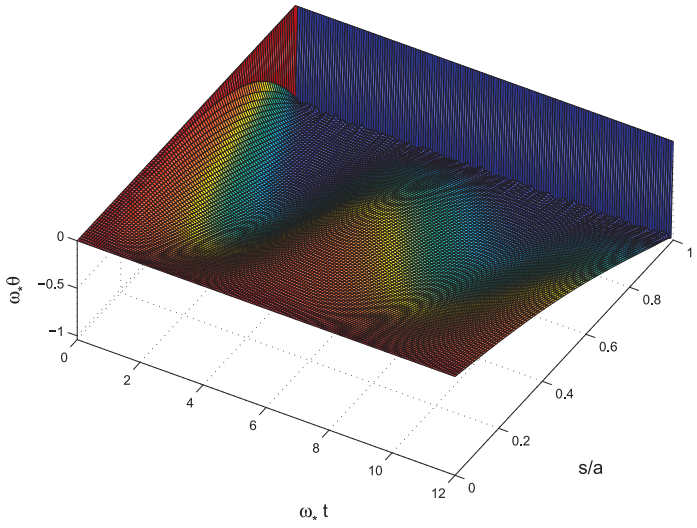

Fig. 7. The dimensionless weight function $\omega_* \theta(s,\, t)$ for $(s, t) \in [0, a] \times \omega_*^{-1}\mathbb{R}^+$.

It appears that $\theta(s,\, t)$ is continuous and continuously differentiable with respect to the time variable t; $\theta(s,\, t)$ is although discontinuous with respect to the space variable at $s = a$ so that both $\omega_* \theta(s,\, t)$ and $D_t\theta(s, t) \equiv \dot{\theta}(s, t)$ vanish at any lattice site $s \in a\mathcal{N}$ for all $t \in \omega_*^{-1}\mathbb{R}$. One can also observe that these dimensionless causal functions tend towards the following long time limits as $\omega_* t$ becomes large

$$\omega_* \theta(s, +\infty) = -\mathbb{1}_{[0,a[}(s)\, \frac{s}{a} \quad \text{and} \quad \dot{\theta}(s, +\infty) = 0, \tag{62}$$

so that $\omega_* |\theta(s, +\infty)|$ measures the fraction of the segment $[0,\, s]$ over the reference lattice distance a, similarly to Hardy's bond function (Hardy, 1982).

Now, in time space, the normal stress values $I_\varepsilon[u](s^\pm,\, t)$ at $(s, t) \in]0, L[\times \omega_*^{-1}\mathbb{R}^+$ are given by

$$\begin{aligned} I_\varepsilon[u](s^-, t) = {} & \alpha \mathrm{H}(t)\, \frac{u(s, t) - u(s - a, t)}{a} + \frac{\rho a}{2}\, D_t^2[\mathrm{H}(t)\, u(s, t)] \\ & + \omega_* a \sum_{p=1}^{N-1} \Big\{ \int_0^t f_p(t - \hat{t})\, D_{\hat{t}}\theta(s_{p+1} - s, \hat{t})\, d\hat{t} \\ & + \rho \left[u_p^o\, D_t^2\theta(s_{p+1} - s, t) + v_p^o\, D_t\theta(s_{p+1} - s, t) \right] \Big\}; \end{aligned} \tag{63a}$$

$$\begin{aligned} I_\varepsilon[u](s^+, t) = {} & \alpha \mathrm{H}(t)\, \frac{u(s + a, t) - u(s, t)}{a} - \frac{\rho a}{2}\, D_t^2[\mathrm{H}(t)\, u(s, t)] \\ & + \omega_* a \sum_{p=1}^{N-1} \Big\{ \int_0^t f_p(t - \hat{t})\, D_{\hat{t}}\theta(s_{p-1} - s, \hat{t})\, d\hat{t} \\ & + \rho \left[u_p^o\, D_t^2\theta(s_{p-1} - s, t) + v_p^o\, D_t\theta(s_{p-1} - s, t) \right] \Big\}. \end{aligned} \tag{63b}$$

Alternatively, in order to see how each atom contributes to that continuum stress at a fixed spatial-time position at $(s, t) \in]0, L[\times \omega_*^{-1}\mathbb{R}^+$ one can also combine the Newton's dynamical equations in (11a) with the equivalence $u(s_k,\, t) \equiv u_k(t)$ for $(k, t) \in \mathcal{N} \times \omega_*^{-1}\mathbb{R}$ and fully express then $I_\varepsilon[u](s^\pm,\, t)$ in terms of the interpolating displacement field $u(s,\, t)$ like

$$\begin{aligned} I_\varepsilon[u](s^-, t) = {} & \alpha \mathrm{H}(t)\, \frac{u(s, t) - u(s - a, t)}{a} + \frac{\rho a}{2}\, D_t^2[\mathrm{H}(t)\, u(s, t)] \\ & + \rho \omega_* a \sum_{p=1}^{N-1} D_t^2 \int_0^t u(s_p, t - \hat{t})\, D_{\hat{t}}\theta(s_{p+1} - s, \hat{t})\, d\hat{t} \\ & - \frac{\alpha \omega_*}{a} \sum_{p=1}^{N-1} \int_0^t \left[u(s_{p+1}, t - \hat{t}) + u(s_{p-1}, t - \hat{t}) - 2u(s_p, t - \hat{t}) \right] \\ & \times D_{\hat{t}}\theta(s_{p+1} - s, \hat{t})\, d\hat{t}; \end{aligned} \tag{64a}$$

$$\begin{aligned} I_\varepsilon[u](s^+, t) = {} & \alpha \mathrm{H}(t)\, \frac{u(s + a, t) - u(s, t)}{a} - \frac{\rho a}{2}\, D_t^2[\mathrm{H}(t)\, u(s, t)] \\ & + \rho \omega_* a \sum_{p=1}^{N-1} D_t^2 \int_0^t u(s_p, t - \hat{t})\, D_{\hat{t}}\theta(s_{p-1} - s, \hat{t})\, d\hat{t} \\ & - \frac{\alpha \omega_*}{a} \sum_{p=1}^{N-1} \int_0^t \left[u(s_{p+1}, t - \hat{t}) + u(s_{p-1}, t - \hat{t}) - 2u(s_p, t - \hat{t}) \right] \\ & \times D_{\hat{t}}\theta(s_{p-1} - s, \hat{t})\, d\hat{t}. \end{aligned} \tag{64b}$$

One observes here then that the time integrals involve a specific average of both the inertial and elastic interaction forces when the stress $I_\varepsilon[u](s,\, t)$ is evaluated at non-material continuum points $s \in \mathcal{S} \setminus (a\mathcal{N})$. These integrals vanish with $D_t\theta$ at the lattice sites $s \in a\mathcal{N}$ so that the prior relations are simpler at the inner lattice sites

$$\begin{aligned} -I_\varepsilon[u](s_k^-, t) = {} & -\alpha \mathrm{H}(t)\, \frac{u(s_k, t) - u(s_{k-1}, t)}{a} \\ & - \frac{\rho a}{2}\, D_t^2[\mathrm{H}(t)\, u(s_k, t)], \quad \text{for } k \in \mathcal{N} \setminus \{0\} \end{aligned} \tag{65a}$$

$$\begin{aligned} I_\varepsilon[u](s_k^+, t) = {} & \alpha \mathrm{H}(t)\, \frac{u(s_{k+1}, t) - u(s_k, t)}{a} \\ & - \frac{\rho a}{2}\, D_t^2[\mathrm{H}(t)\, u(s_k, t)], \quad \text{for } k \in \mathcal{N} \setminus \{N\} \end{aligned} \tag{65b}$$

or again by using notably the Newton's equations in (10) while $u(s_k,\, t) \equiv u_k(t)$ for $k \in \mathcal{N}$

$$\begin{aligned} -I_\varepsilon[u](s_k^-, t) = {} & -\alpha\, \mathrm{H}(t) \left[\frac{u(s_{k+1}, t) - u(s_k, t)}{2a} \right. \\ & \left. + \frac{u(s_k, t) - u(s_{k-1}, t)}{2a} \right] \\ & - \frac{a}{2} \left[f_k(t) + \rho\, \mathfrak{D}_t^2 u_k(t) \right], \quad \text{for } k \in \mathcal{N} \setminus \{0\}; \end{aligned} \tag{66a}$$

$$\begin{aligned} I_\varepsilon[u](s_k^+, t) = {} & \alpha\, \mathrm{H}(t) \left[\frac{u(s_{k+1}, t) - u(s_k, t)}{2a} + \frac{u(s_k, t) - u(s_{k-1}, t)}{2a} \right] \\ & - \frac{a}{2} \left[f_k(t) + \rho\, \mathfrak{D}_t^2 u_k(t) \right], \quad \text{for } k \in \mathcal{N} \setminus \{N\}. \end{aligned} \tag{66b}$$

All these equivalent (material law) expressions have in fact one meaningful interpretation, which extends the Cauchy's classical mechanics concept of *internal traction force resultant* (or vector) that acts on any material interface in a way that somewhat differs from Cheung and Yip (1991) and Tsai's atomic-level mechanical stress ones (Tsai, 1979) but agrees with other deductions regarding the traction forces in a cell of two half-particles connected by a massless bond (see Slepyan 2002, page 88). Indeed, $-I_\varepsilon[u](s_k^-, t)$ (respectively $I_\varepsilon[u](s_k^+, t)$) can be interpreted from Eqs. (65) as a generalisation of the *internal traction force resultant* (vector) that is exerted by the material points with labels $p \le k$ (resp. $p \ge k$) onto the (Euler-Bernoulli's) cut plane that permanently splits the k^{th} moving atom into two equal masses $\rho a/2$ (as illustrated in Fig. 8), unlike the fixed spatial/geometric dividing surface used by

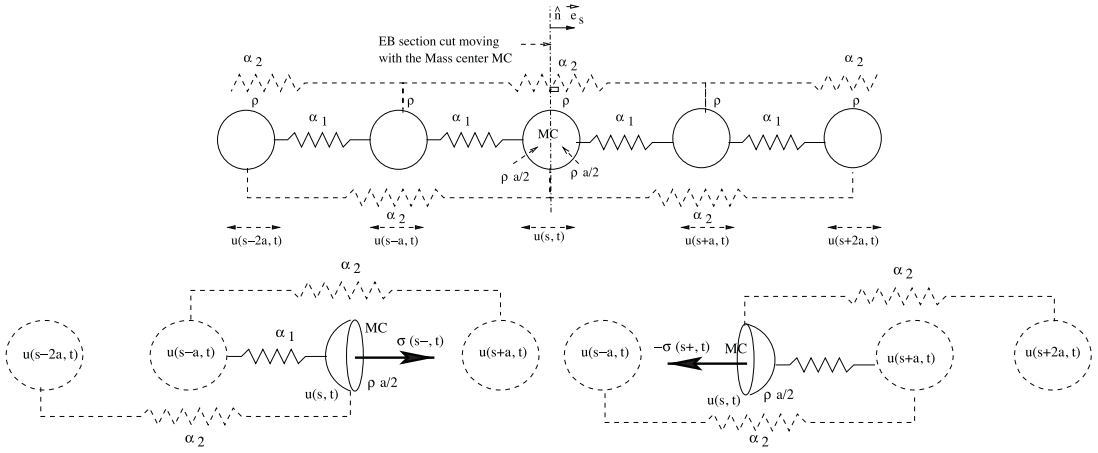

Fig. 8. Interpretation of the inertial contribution $\mp\frac{\rho a}{2}D_t^2u(s_k,t)$ into the normal stress $\sigma(s_k^{\pm},t)\overset{\text{def}}{=}I_\varepsilon[u](s_k^{\pm},t)$ at the atomic level. This schemas also suggests with dashed lines next-nearest neighbor elastic interactions (**NNNI**) (*with two types of spring constants* $\alpha_1\equiv\alpha$ *and* α_2), which were treated in quasistatics in Charlotte (2001); Charlotte and Truskinovsky (2002, 2008). For the NNNI monatomic case, the cut section at s_k undergoes the loads of one spring constant α_1 and two spring constants α_2, which must balanced with the appropriate normal cohesive force $\mp\sigma(s_k^{\pm},t)$ and inertial loads $\mp\frac{\rho a}{2}D_t^2u(s_k,t)$ accordingly with D'Alembert's principle. That stress notion agrees with Cauchy's and Saint-Venant's original definition for stress vector (or traction) if formulated as in Ref. (Timoshenko, 1983).

Gibbs (1928), Tsai (1979), Cheung and Yip (1991). Here while the splitting plane moves with the particle displacement $u_k(t)$ in lagrangian description, each equation in (65) merely expresses in absence of spatially concentrated external forces af_k the dynamic balance for one of the two neighboring solids with mass $\rho a/2$, while more generally the ensuing standard jump relations for the traction forces on the internal interfaces arise

$$I_\varepsilon[u](s_k^+,t)-I_\varepsilon[u](s_k^-,t)\equiv-a\Big[f_k(t)+\rho\,\mathfrak{D}_t^2u_k(t)\Big] \tag{67}$$

for $(s_k,t)=(ka,t)\in a(\mathcal{N}\setminus\{0,N\})\times\omega_*^{-1}\mathbb{R}$. Actually, the jump relation in (67) can also be extended to the particles at the chain ends $s_0=0$ and $s_N=Na=L$ as suggested by Eqs. (46) and (47). This interpretation and the boundary conditions with surface inertial pressures in (47) suggest a slight analogy with Zwanzig's mechanical modeling of atom/solid-surface inelastic scattering (Zwanzig, 1960), as well as (Adelman and Doll, 1974, 1976), and Mori's works (Mori, 1965) on the *generalized Langevin equations* (see also (Tadmor and E., 2007, 2008; Español, 1996)). In his work, Zwanzig assumes that only the outer atom of the chain interacts directly with the impinging particle of gasand then derives an equation of motion for the scattering process which does not explicitly include the coordinates of the remaining atoms of the chain. In the TC PC description, such interactions are considered to occur with the outer half-masses of the chain.

It is lately worth emphasizing before concluding that all the relations that were previously given for the particle in the chain bulk domain also hold for the infinite domain case $\mathcal{N}=\mathbb{Z}$ analyzed in Charlotte and Truskinovsky (2012) (as well as at the free moving atoms of a finite chain submitted to Dirichlet boundary conditions). Ratios like

$$\frac{-I_\varepsilon[\hat u](s_k^-,\omega)}{i\omega\hat u(s_k,\omega)}\quad\text{and}\quad\frac{I_\varepsilon[\hat u](s_{k-1}^+,\omega)}{i\omega\hat u(s_{k-1},\omega)}$$

that are computed with Eq. (65) and traveling monochromatic waves like $\hat u(s_k,t)\sim e^{\pm i[\omega t\pm\lambda_0(\omega)s_k]}$ are analogs of the characteristic (mechanical) impedances used by Brillouin and Parodi's one (Brillouin and Parodi, 1956, chap. 5, sec. 22, page 86) in their reflectionless interfacial conditions. Eqs. (46), (47) and (65) outline however a more comprehensive way for linking continuum local stress field notions with interaction forces in the lattice models.

5. Concluding remarks and perspectives

The construction of enriched continuum models from molecular dynamics models, possibly for a coupling or a substitution, requires dealing with the terms of inertia and stiffness, length scales and time intrinsic structures and finally adopting the most relevant ingredients. At the same time, it seems of practical interest that these continuum models exhibit some relationships with the molecular forces and the concept of stress at the atomic level. The twofold objective of this study (as an extension to the work in Charlotte and Truskinovsky (2012)) was therefore to construct such an enriched continuum model whose solutions provide an *exact interpolation* of a finite lattice model dynamics, with an interpretation of the discrete atomistic forces and deformation into continuum (normal) stress and (normal) strain fields maintaining the physical effects of the atomistic system. This pseudocontinuum achievement was obtained by focusing on a simple nonlocality and a dispersion relation, while excluding the effects of nonlinearity and inter-particle collision but by allowing however concentrate and impact loads. The geometric and structural complexity of the problem was also minimized by focusing on the simplest 1D chain with nearest neighbor interactions. A dynamic mechanical analysis was used then to exhibit a pseudocontinuum model with a bounded domain, nontrivial inertia and hereditary elasticity (temporally nonlocal or TN PC model), which accomplishes an exact interpolation of the prototypical discrete model. This extends so the framework of continuum mechanics to the spatial and temporal scales where the behavior of a crystal lattice is highly discrete and those describing the geometry and loading are comparable to their internal counterparts and dictated by the lattice/granular system itself.

Interestingly, the unusual non-Newtonian inertia of the TN PC model (see Section 3) can also be understood in the framework of a meta-material paradigm (Milton and Willis, 2007; Willis, 1981; Willis and Suquet, 1997) which presumes that a "visible" continuum particle carries a variety of internal degrees of freedom representing locally non-affine (non Cauchy-Born) dynamic responses. The hereditary/memory structure of the TN PC elasticity can be linked to the "structural attenuation" (Brillouin and Parodi, 1956) involving energy redistributions between macroscopic to microscopic degrees of freedom. In this sense, the non-classical inertia and the hereditary/memory structure of elasticity are the means of adequate continuum representation of high frequency vibrations

of the lattice without introducing temperature (see also Adelman and Doll, 1974, 1976; Karpov et al., 2007; Mauricio and Velasco, 1984; Park et al., 2005; Park and Liu, 2004; Tadmor and Miller, 2011; Tadmor and E., 2007, 2008; Tang et al., 2006). This allows the presence of a classical inertial contribution (in the sense of D'Alembert, in a lagrangian description) into the simple atomistic definition of the TN PC normal stress component like in (65). This inertial contribution appears to be in agreement with the continuum definition of stress that is stated solely in terms of the forces acting between different parts of the body (Timoshenko, 1983). This interpretation differs from the kinetic *virial stress* model (Admal and Tadmor, 2010) inspired by Clausius' work (Clausius, 1870), which has led to controversy in the past (Zhou, 2003). However, as suggested by the more complex formulas in (64) outside of the lattice sites $a\mathcal{N}$, the continuum governing equations of motion involving such a stress field must be associated with non-trivial inertial forces instead of the usual Newtonian one $-\rho D_t^2 u$ as shown in Section 3. It should not be overlooked that the involved time derivative corresponds to the material one. Although this interpretation seems to be new, similar discrete formulas as the one in (65) had already been conjectured by Cheung and Yip (1991) for the Cauchy's stress term as a correction of Tsai's original ideas (Tsai, 1979). Nevertheless, in spite of their numerical proof for a model system of bcc iron, Cheung and Yip's heuristic formulation appeared with an analytical derivation and embedded a number of oddities according to (Zimmerman et al., 2002, Chap. 4,Sec.4.2), like in fact the misleading use of a momentum transport across a *spatial/geometric* description of Gibbs' dividing surface (*i.e.*the Euler-Bernoulli's cut-plane) instead of a *material* one that is tied to a half-mass moving particle.

Extensions of this atomistic definition may be useful for the multiscale modeling of material behavior which combines both lattice system with simple microstructures and continuum descriptions in the development of constitutive relations at different scales to link the MD and continuum descriptions. Albeit the atomistic definition may be easily adapted, the unquestionable complexity of the derivation techniques of the TN equations makes it hardly practicable outside some particularly simple one-dimensional dynamic situations. The extension of the proposed model towards including interactions beyond nearest neighbors seems to be straightforward in view of the results obtained in Charlotte (2001); Charlotte and Truskinovsky (2002, 2008) and will require adding appropriate internal variables equipped with their own temporal and spatial non-locality. Similar derivations for non-simple lattices and periodic material systems, representing Cosserat's media (Suiker and de Borst, 2005; Suiker et al., 2001) or granular metamaterials, and for which the use nonlocal spatial, multifield theories (Il'iushina, 1969; see also the various contributions in Kroner, 1968) become necessary to describe the fine micro-structural behaviors, are currently under investigation. Nevertheless, the present derivation techniques are obviously less straightforward to implement in higher dimensions and for anisotropic structures. So it should be addressed in a phenomenological way, by considering the main singular spectral features of the discrete models. As a simple solution, the enrichment may be limited to the domain boundary. The benefits of such a localized enrichment will be illustrated in a forthcoming communication for the D'Alembert's string/rod model.

Appendix A. The model Green function

This section provides the explicit expressions of the continuous kernel $G(s,\hat{s},t)$ introduced in (28) with some of its properties. The formulas notably involve two length scales $\ell_-(\omega)$ (for $\omega\in[-\omega_*,\omega_*]$) and $\ell_+(\omega)$ (for $\omega\in\omega_*\mathbb{R}\setminus[-\omega_*,\omega_*]$) introduced in Eqs. (24a) and (24b) to describe respectively the properties of wave-dispersion and wave-attenuation (Brillouin and Parodi, 1956; Charlotte and Truskinovsky, 2012) with respect to the wave frequencies.

A simple application of the Cauchy's theorem of residues over the reduced complex domain $\omega_*\mathbb{C}\setminus\mathcal{C}$ provides

$$G(s,\hat{s},t)-G_{\rm K}(s,\hat{s},t)\equiv\frac{4\,{\rm H}(t)}{\pi\,\omega_*^2}\int_{\omega_*}^{\infty}\sin(\omega_r t)\times\left[\frac{\sin(\frac{\pi\,|s-\hat{s}|}{a})\,\sinh(\frac{L-|s-\hat{s}|+a}{\ell_+})}{\sinh(\frac{a}{\ell_+})\,\sinh(\frac{L+a}{\ell_+})}-\frac{\sin(\frac{\pi\,(s+\hat{s})}{a})\,\sinh(\frac{L-s-\hat{s}}{\ell_+})}{\sinh(\frac{a}{\ell_+})\,\sinh(\frac{L+a}{\ell_+})}\right]d\omega_r. \tag{A.1}$$

This result involves the following kernel

$$G_{\rm K}(s,\hat{s},t)\stackrel{\rm def}{=}\frac{{\rm H}(t)}{N+1}\left\{t+\sum_{p=1}^{N}\frac{\sin(\omega_p t)}{\omega_p}\left[\frac{\cos(\lambda_{o,p}\,(L-|s-\hat{s}|+a))}{\cos((L+a)\lambda_{o,p})}+\frac{\cos(\lambda_{o,p}\,(L-s-\hat{s}))}{\cos((L+a)\lambda_{o,p})}\right]\right\}, \tag{A.2a}$$

which can also be read as the following trigonometric polynomials

$$G_{\rm K}(s,\hat{s},t)\equiv\frac{{\rm H}(t)}{N+1}\sum_{p\in\mathcal{N}}(2-\delta_{p,0})\,\mathcal{F}_p(s)\,\mathcal{F}_p(\hat{s})\,t\,{\rm sinc}(\omega_p t/\pi) \tag{A.2b}$$

with

$${\rm sinc}(\eta)\stackrel{\rm def}{=}\frac{\sin(\pi\,\eta)}{\pi\,\eta},\ \text{for}\ \eta\in\mathbb{R} \tag{A.3}$$

while

$$\lambda_{o,p}\stackrel{\rm def}{=}\frac{p\pi}{L+a},\ \omega_p\stackrel{\rm def}{=}\omega_*\sin(\lambda_{o,p}a/2)\ \text{ and }\ \mathcal{F}_p(s)\stackrel{\rm def}{=}\cos\big(\lambda_{o,p}(s+a/2)\big),\ \text{for}\ p\in\mathcal{N}. \tag{A.4}$$

Here $\mathcal{F}_p(s)$ represents spatially-periodic "monochromatic wave" function of deformation whose the wavelength $\lambda_{o,p}^{-1}$ can also be related to the angular modal frequency ω_p in (A.4) like $\lambda_{o,p}^{-1}\equiv[\lambda_o(-\omega_p)]^{-1}\equiv\ell_-(\omega_p)$. Each couple $(\omega_p,\boldsymbol{\mathcal{F}}_p\stackrel{\rm def}{=}\{\mathcal{F}_p(ka)\}_{k\in\mathcal{N}})$ (for $p\in\mathcal{N}$) notably represents a *normal mode of vibration* satisfying the homogeneous self-adjoint Eigen-value problem of the lattice dynamic problem considered in Section 2

$$-\rho\,\omega_p^2\,\mathcal{F}_p(ka)=\frac{\alpha}{a^2}\Big\{\big[\mathcal{F}_p(ka+a)-\mathcal{F}_p(ka)\big](1-\delta_{k,N})+\big[\mathcal{F}_p(ka-a)-\mathcal{F}_p(ka)\big](1-\delta_{k,0})\Big\},\ \text{for}\ k\in\mathcal{N}.$$

The equivalence in (A.2b), that more specifically requires

$$\frac{\cos((L-|s-\hat{s}|+a)\lambda_{o,p})+\cos((L-s-\hat{s})\lambda_{o,p})}{\cos((L+a)\lambda_{o,p})}\equiv 2\cos((s+a/2)\lambda_{o,p})\cos((\hat{s}+a/2)\lambda_{o,p})$$

for any couple $(s,\hat{s})\in a\mathbb{R}^2$, holds because for any $\lambda\in a^{-1}\mathbb{C}$

$$2\cos((s+a/2)\lambda)\cos((\hat{s}+a/2)\lambda)\equiv\cos((s-\hat{s})\lambda)+\cos((s+\hat{s}+a)\lambda)$$

and then for any $(L+a)\lambda\in\pi\mathbb{Z}$

$$\sin((L+a)\lambda)=0$$

$$\cos((s-\hat{s})\lambda)+\cos((s+\hat{s}+a)\lambda)\equiv\frac{\cos((L-|s-\hat{s}|+a)\lambda)+\cos((L-s-\hat{s})\lambda)}{\cos((L+a)\lambda)}.$$

It is worth mentioning that mathematically, for the state space formed by the discrete displacements $\boldsymbol{u}(t)=\{u(t)\}_{k\in\mathcal{N}}$ and momenta $\rho D_t\boldsymbol{u}(t)\equiv\rho\dot{\boldsymbol{u}}(t)=\{\rho\dot{u}(t)\}_{k\in\mathcal{N}}$ of our discrete system of N

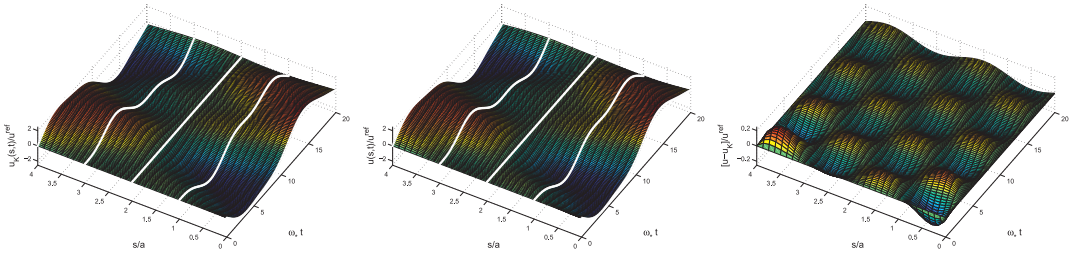

(a) Impact response G_{K} (b) Impact response G (c) Impact response fluctuation $G - G_{\mathrm{K}}$

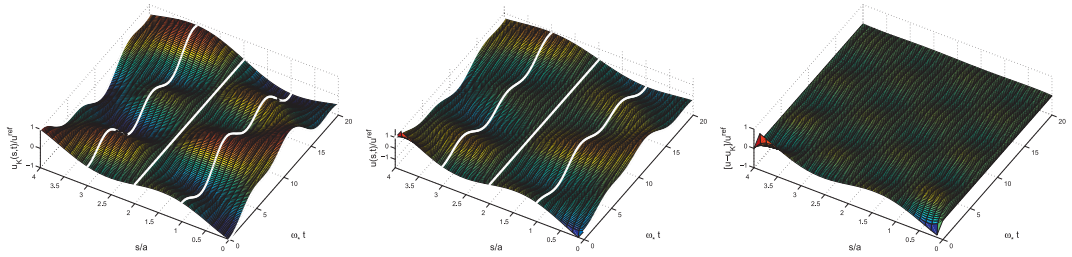

(d) Release response $D_t G_{\mathrm{K}}$ (e) Release response $D_t G$ (f) Release response fluctuation $D_t G - D_t G_{\mathrm{K}}$

Fig. A-9. Decompositions of the impact (top) and release (bottom) test responses for $t \in [0, T^*]$ and $N = L/a = 4$: interpolations of the $(N+1)$-atomic displacements $\boldsymbol{u}(t)$.

atoms, the set $\{\mathcal{F}_p\}_{p\in\mathcal{N}}$ forms a *complete set* of *orthonormal basis states* with respect to some scalar products so that all "physical observables" such like the discrete displacements $\boldsymbol{u}(t) = \{u(t)\}_{k\in\mathcal{N}}$ and momenta $\rho D_t \boldsymbol{u}(t) \equiv \rho\dot{\boldsymbol{u}}(t) = \{\rho\dot{u}(t)\}_{k\in\mathcal{N}}$, and the total mechanical Hamiltonian energy of the chain can be expressed. These eigenstates can also be associated with pseudocontinuum Hamiltonian representations (with specific field restrictions), what will be expanded in subsequent articles. Here their contributions in G_{K} and $D_t G_{\mathrm{K}}$ as well as the damping fluctuations $G - G_{\mathrm{K}}$ and $Dt[G - G_{\mathrm{K}}]$ are illustrated in Fig. A-9 for the impact and release responses $u(s, t)$ presented in Fig. 6 and also again for convenience in Figs. A-9(b) and A-9(e). The additional effects that TN PC tries to account for, introduce the non-conservative contributions in the physical observables such like the displacements (and measurable quantities such like) stress and works. Without the attenuation part in the expression of the impulse response (or Greens function) of the TN PC, the part associated to propagating waves can be related to a spatially-nonlocal Hamiltonian model, with however some modifications for the definition of the material domain (topology and elasticity).

Appendix B. Derivation of the TN equations

That section derives the IBVP that satisfies the symmetric interpolating kernel $G(s, \hat{s}, t) \equiv G(\hat{s}, s, t)$ and that lead to the appropriate expressions for $I_1[\,\cdot\,](s, t)$, $I_\varepsilon[\,\cdot\,](s, t)$ and $I_p^{\mathrm{surf}}[\cdot](s, t)$. Indeed it raises that, in addition to Eqs. (19a) and (20), the expression of $G(s, \hat{s}, \omega) \equiv G(\hat{s}, s, \omega)$ in Eq. (21) also satisfies

$$-\alpha \frac{\sin\left(\lambda_o(\omega)a\right)}{\lambda_o(\omega)a}\left[D_s^2 G(s, \hat{s}, \omega) + \lambda_o^2(\omega) G(s, \hat{s}, \omega)\right] = \rho a \delta(s - \hat{s}), \quad \text{for } (s, \hat{s}) \in (a\mathbb{R})^2 \tag{B.1a}$$

with at the extremities of the domain $\mathcal{S}$ subjected to Robin's boundary conditions

$$\alpha \frac{\sin\left(\lambda_o(\omega)a\right)}{\lambda_o(\omega)a} D_s G(s, \hat{s}, \omega) = \frac{\rho a \omega^2}{2} G(s, \hat{s}, \omega), \quad \text{for } s = 0^- < \hat{s} \in \mathcal{S} \tag{B.1b}$$

$$\alpha \frac{\sin\left(\lambda_o(\omega)a\right)}{\lambda_o(\omega)a} D_s G(s, \hat{s}, \omega) = -\frac{\rho a \omega^2}{2} G(s, \hat{s}, \omega), \quad \text{for } s = L^+ > \hat{s} \in \mathcal{S}. \tag{B.1c}$$

These relations are notably obtained by using $\cos\left(\lambda_o(\omega)a\right) = 1 - 2\dfrac{\omega^2}{\omega_*^2}$ and $\rho\omega_*^2 a^2 = 4\alpha$ and the following formulas for $(s, \hat{s}) \in (a\mathbb{R}) \times (a\mathbb{R} \setminus \{s\})$

$$D_s G(s, \hat{s}, \omega) = -\frac{\rho a^2 \lambda_o(\omega)}{2\alpha} \times \frac{\operatorname{sgn}(s - \hat{s}) \sin\left(\lambda_o(\omega)(L - |s - \hat{s}| + a)\right) + \sin\left(\lambda_o(\omega)(L - s - \hat{s})\right)}{\sin\left(\lambda_o(\omega)a\right) \sin\left(\lambda_o(\omega)(L + a)\right)}$$

$$D_s G(s, s^+, \omega) = D_s G(s, s^-, \omega) + \frac{\rho a^2 \lambda_o(\omega)}{\alpha \sin\left(\lambda_o(\omega)a\right)}$$

$$D_s G(\hat{s}^+, \hat{s}, \omega) = D_s G(\hat{s}^-, \hat{s}, \omega) - \frac{\rho a^2 \lambda_o(\omega)}{\alpha \sin\left(\lambda_o(\omega)a\right)}$$

$$D_{\hat{s}}^2 G(s, \hat{s}, \omega) = -\frac{\rho a^2}{\alpha} \frac{\lambda_o(\omega)}{\sin\left(\lambda_o(\omega)a\right)} \delta(s - \hat{s}) - \lambda_o^2(\omega) G(s, \hat{s}, \omega).$$

The properties in (B.1) for $G(s, \hat{s}, \omega)$ (while $\omega \in \omega_* \mathbb{C}$ with $\Im m(\omega) < -\breve{\omega}_b \leq 0$) specify in LT spectral analysis terms that the BVP for the TN PC must be settled with

$$I_1[G](s, \hat{s}, \omega) \stackrel{\text{def}}{=} -\alpha \frac{\sin\left(\lambda_o(\omega)a\right)}{\lambda_o(\omega)a} \lambda_o^2(\omega) G(s, \hat{s}, \omega), \quad \text{for } (s, \hat{s}) \in]0, L[\times \mathcal{S} \tag{B.2a}$$

$$I_\varepsilon[G](s,\hat{s},\omega) \stackrel{\text{def}}{=} \alpha \frac{\sin\left(\lambda_o(\omega)a\right)}{\lambda_o(\omega)a} D_s G(s,\hat{s},\omega), \text{ for } (s,\hat{s}) \in]0,L[\times\mathcal{S} \tag{B.2b}$$

$$I_p^{\text{surf}}[G](s,\hat{s},\omega) \stackrel{\text{def}}{=} -\frac{\rho a\omega^2}{2} G(s,\hat{s},\omega), \text{ for } (s,\hat{s}) \in \{0,L\}\times\mathcal{S}. \tag{B.2c}$$

Hence, according to that dynamical mechanical analysis, the ansatz formulated in Eq. (36) must involve a bulk integro-differential governing equation like

$$I_1[G](s,\hat{s},t) - D_s I_\varepsilon[G](s,\hat{s},t) = \rho\, a\, \delta(s-\hat{s})\,\delta_+(t), \quad \text{for } (s,\hat{s},t) \in (a\mathbb{R})^2 \times \omega_*^{-1}\mathbb{R}, \tag{B.3a}$$

pre-initial conditions like

$$G(s,\hat{s},t) = 0, \text{ for } (s,\hat{s},t) \in (a\mathbb{R})^2 \times \omega_*^{-1}\mathbb{R}^- \tag{B.3b}$$

and naturally, but nontrivially, Robin-like boundary conditions

$$I_p^{\text{surf}}[G](0,0,t) - I_\varepsilon[G](0^+,0,t) = \rho\, a\, \delta_+(t), \tag{B.3c}$$

$$I_p^{\text{surf}}[G](L,L,t) + I_\varepsilon[G](L^-,L,t) = \rho\, a\, \delta_+(t), \tag{B.3d}$$

while for $(\hat{s},t) \in (\mathcal{S}\setminus\{0,L\})\times\omega_*^{-1}\mathbb{R}$

$$I_p^{\text{surf}}[G](0,\hat{s},t) \equiv I_\varepsilon[G](0^-,\hat{s},t) \equiv I_\varepsilon[G](0,\hat{s},t) \tag{B.3e}$$

$$I_p^{\text{surf}}[G](L,\hat{s},t) \equiv -I_\varepsilon[G](L^+,\hat{s},t) \equiv -I_\varepsilon[G](L,\hat{s},t). \tag{B.3f}$$

Finally, the identifications in (B.2) can now be expressed explicitly in time-variable for u, based notably on the linearity of the problem model in (36).

Appendix C. Energy of the atomic chain under impacts

This section provides the expression for the work done by the related generalized load in (4)

$$\boldsymbol{f}(t) = \boldsymbol{f}^r(t) + \boldsymbol{f}^i(t) \text{ with } \boldsymbol{f}^r(t) = \left\{\tilde{f}_k(t)\right\}_{k\in\mathcal{N}},$$
$$\boldsymbol{f}^i(t) = \left\{\sum_{t_p\in\mathcal{T}_1[f_k](t)} \bar{p}_k(t)\delta_+(t-t_p)\right\}_{k\in\mathcal{N}} \tag{C.1}$$

in the *continuous* displacements $\boldsymbol{u}$ in (26). Using the regularizing limit process described in (8) with

$$af_k^\epsilon(t) = a\tilde{f}_k(t) + \sum_{t_p\in\mathcal{T}_1[f_k](t)} \bar{p}_k(t_p)\,\frac{\mathrm{H}(t-t_p)-\mathrm{H}(t-t_p-\epsilon)}{\epsilon} \tag{C.2}$$

so that

$$\lim_{\epsilon\searrow 0} af_k^\epsilon(t) \equiv af_k(t) = a\tilde{f}_k(t) + \sum_{t_p\in\mathcal{T}_1[f_k](t)} \bar{p}_k(t_p)\delta_+(t-t_p), \tag{C.3}$$

we get indeed then for the displacements as given by the generic expression in (26)

$$u_k^\epsilon(t) = \sum_{j\in\mathcal{N}}\Big[\int_0^t G(ka,ja,t-\hat{t})\frac{f_j^\epsilon(\hat{t})}{\rho}d\hat{t} + D_t\widehat{G}(ka,ja,t)u_j^o + \widehat{G}(ka,ja,t)v_j^o\Big] \tag{C.4}$$

for $(k,t)\in\mathcal{N}\times\omega_*^{-1}\mathbb{R}$. This expression can be simplified successively as follows

$$\begin{aligned}
u_k^\epsilon(t) &= \sum_{j\in\mathcal{N}}\Big[\int_0^t G(ka,ja,t-\hat{t})\frac{a\tilde{f}_j(\hat{t})}{\rho}\,d\hat{t} + \dot{\widehat{G}}(ka,ja,t)u_j^o \\
&\quad + \widehat{G}(ka,ja,t)v_j^o\Big] \\
&\quad + \sum_{j\in\mathcal{N}}\int_0^t G(ka,ja,t-\hat{t}) \\
&\quad \times\Big[\sum_{t_p\in\mathcal{T}_1[f_k](\hat{t})}\frac{\bar{p}_j(t_p)}{\rho}\,\frac{\mathrm{H}(\hat{t}-t_p)-\mathrm{H}(\hat{t}-t_p-\epsilon)}{\epsilon}\Big]d\hat{t} \\
&= \sum_{j\in\mathcal{N}}\Big[\int_0^t G(ka,ja,t-\hat{t})\frac{a\tilde{f}_j(\hat{t})}{\rho}d\hat{t} + \dot{\widehat{G}}(ka,ja,t)u_j^o \\
&\quad + \widehat{G}(ka,ja,t)v_j^o\Big] \\
&\quad + \sum_{(j,t_p)\in\mathcal{N}\times\mathcal{T}_1[f_k](t)}\frac{\bar{p}_j(t_p)}{\rho}\Big[\frac{\mathrm{H}(t-t_p)}{\epsilon}\int_{t_p}^t G(ka,ja,t-\hat{t})d\hat{t} \\
&\quad - \frac{\mathrm{H}(t-t_p-\epsilon)}{\epsilon}\int_{t_p+\epsilon}^t G(ka,ja,t-\hat{t})d\hat{t}\Big] \\
&= \sum_{j\in\mathcal{N}}\Big[\int_0^t G(ka,ja,t-\hat{t})\frac{a\tilde{f}_j(\hat{t})}{\rho}d\hat{t} + \dot{\widehat{G}}(ka,ja,t)u_j^o \\
&\quad + \widehat{G}(ka,ja,t)v_j^o\Big] \\
&\quad + \sum_{(j,t_p)\in\mathcal{N}\times\mathcal{T}_1[f_k](t)}\frac{\bar{p}_j(t_p)}{\rho}\Big[\frac{\mathrm{H}(t-t_p)-\mathrm{H}(t-t_p-\epsilon)}{\epsilon} \\
&\quad \times\int_{t_p}^t G(ka,ja,t-\hat{t})d\hat{t} \\
&\quad + \frac{\mathrm{H}(t-t_p-\epsilon)}{\epsilon}\int_{t_p}^{t_p+\epsilon} G(ka,ja,t-\hat{t})d\hat{t}\Big]
\end{aligned} \tag{C.5}$$

that last formulas giving consecutively the velocity for $t>0$

$$\begin{aligned}
\dot{u}_k^\epsilon(t) &= \sum_{j\in\mathcal{N}}\Big[\int_0^t \dot{G}(ka,ja,t-\hat{t})\frac{a\tilde{f}_j(\hat{t})}{\rho}d\hat{t} \\
&\quad + \ddot{\widehat{G}}(ka,ja,t)u_j^o + \dot{\widehat{G}}(ka,ja,t)v_j^o\Big] \\
&\quad + \sum_{(j,t_p)\in\mathcal{N}\times\mathcal{T}_1[f_k](t)}\frac{\bar{p}_j(t_p)}{\rho}\Big[\frac{\mathrm{H}(t-t_p)-\mathrm{H}(t-t_p-\epsilon)}{\epsilon} \\
&\quad \times\int_{t_p}^t \dot{G}(ka,ja,t-\hat{t})d\hat{t} \\
&\quad + \frac{\mathrm{H}(t-t_p-\epsilon)}{\epsilon}\int_{t_p}^{t_p+\epsilon}\dot{G}(ka,ja,t-\hat{t})d\hat{t}\Big]
\end{aligned} \tag{C.6}$$

owing to the properties of the kernels $G(\,\cdot,\,\cdot,t)$ and $\widehat{G}(\cdot,\cdot,t)$ for $t\in\omega_*\mathbb{R}$ and their derivatives. As important features, both the displacement $\boldsymbol{u}^\epsilon(t)$ for $t\geq 0$ and the related velocity $\dot{\boldsymbol{u}}^\epsilon(t)$ for $t>0$ are continuous. Moreover, as $\epsilon\searrow 0^+$, their components converge uniformly respectively towards the following continuous displacement function for $t\geq 0$

$$\begin{aligned}
u_k(t) &= \sum_{j\in\mathcal{N}}\Big[\int_0^t G(ka,ja,t-\hat{t})\frac{a\tilde{f}_j(\hat{t})}{\rho}d\hat{t} \\
&\quad + \sum_{t_p\in\mathcal{T}_1[f_k](t)}\frac{\bar{p}_j(t_p)}{\rho}G(ka,ja,t-t_p) \\
&\quad + \dot{\widehat{G}}(ka,ja,t)u_j^o + \widehat{G}(ka,ja,t)v_j^o\Big]
\end{aligned} \tag{C.7}$$

and the related continuous velocity for $t > 0$

$$\dot{u}_k(t) = \sum_{j\in\mathcal{N}}\Big[\int_0^t \dot{G}(ka, ja, t-\hat{t})\frac{a\tilde{f}_j(\hat{t})}{\rho}d\hat{t} + \sum_{t_p\in\mathcal{T}_l[f_k](t)}\frac{\bar{p}_j(t_p)}{\rho}\dot{G}(ka, ja, t-t_p) + \ddot{\hat{G}}(ka, ja, t)u_j^o + \dot{\hat{G}}(ka, ja, t)v_j^o\Big]. \tag{C.8}$$

Performing the regularized computational limit process for the external work

$$\mathcal{P}_g[\boldsymbol{f},\boldsymbol{u}](t) \overset{\text{def}}{=} \lim_{\epsilon\searrow 0}\mathcal{P}_r[\boldsymbol{f}^\epsilon,\boldsymbol{u}^\epsilon](t) \text{ with } \mathcal{P}_r[\boldsymbol{f}^\epsilon,\boldsymbol{u}^\epsilon](t) \overset{\text{def}}{=} \int_0^t\sum_{k\in\mathcal{N}} af_k^\epsilon(\check{t})\,\dot{u}_k^\epsilon(\check{t})\,d\check{t}$$

gives successively

$$\begin{aligned}\mathcal{P}_g[\boldsymbol{f},\boldsymbol{u}](t) &\equiv \lim_{\epsilon\searrow 0}\int_0^t\sum_{k\in\mathcal{N}}\Big[a\tilde{f}_k(\check{t}) + \sum_{t_p\in\mathcal{T}_l[f_k](\check{t})}\bar{p}_k(t_p)\,\frac{\mathrm{H}(\check{t}-t_p)-\mathrm{H}(\check{t}-t_p-\epsilon)}{\epsilon}\Big]\dot{u}_k^\epsilon(\check{t})\,d\check{t}\\ &\equiv \mathcal{P}_g[\boldsymbol{f}^r,\boldsymbol{u}](t)+\mathcal{P}_g[\boldsymbol{f}^i,\boldsymbol{u}](t)\end{aligned} \tag{C.9}$$

where obviously

$$\mathcal{P}_g[\boldsymbol{f}^r,\boldsymbol{u}](t) = \lim_{\epsilon\searrow 0}\mathcal{P}_r[\tilde{\boldsymbol{f}},\boldsymbol{u}^\epsilon](t) \equiv \lim_{\epsilon\searrow 0}\int_0^t\sum_{k\in\mathcal{N}} a\tilde{f}_k(\check{t})\,\dot{u}_k^\epsilon(\check{t})\,d\check{t}$$

while

$$\begin{aligned}\mathcal{P}_g[\boldsymbol{f}^i,\boldsymbol{u}](t) &= \lim_{\epsilon\searrow 0}\sum_{(k,t_p)\in\mathcal{N}\times\mathcal{T}_l[f_k](t)}\bar{p}_k(t_p)\Big[\frac{\mathrm{H}(t-t_p)}{\epsilon}\int_{t_p}^t\dot{u}_k^\epsilon(\check{t})\,d\check{t} - \frac{\mathrm{H}(t-t_p-\epsilon)}{\epsilon}\int_{t_p+\epsilon}^t\dot{u}_k^\epsilon(\check{t})\,d\check{t}\Big]\\ &\equiv \lim_{\epsilon\searrow 0}\sum_{(k,t_p)\in\mathcal{N}\times\mathcal{T}_l[f_k](t)}\bar{p}_k(t_p)\Big[\frac{\mathrm{H}(t-t_p)-\mathrm{H}(t-t_p-\epsilon)}{\epsilon}\int_{t_p}^t\dot{u}_k^\epsilon(\check{t})\,d\check{t} + \frac{\mathrm{H}(t-t_p-\epsilon)}{\epsilon}\int_{t_p}^{t_p+\epsilon}\dot{u}_k^\epsilon(\check{t})\,d\check{t}\Big]\\ &\equiv \sum_{(k,t_p)\in\mathcal{N}\times\mathcal{T}_l[f_k](t)}\bar{p}_k(t_p)\lim_{\epsilon\searrow 0}\Big\{\frac{\mathrm{H}(t-t_p)-\mathrm{H}(t-t_p-\epsilon)}{\epsilon}\times\big[u_k^\epsilon(t)-u_k^\epsilon(t_p)\big] + \mathrm{H}(t-t_p-\epsilon)\Big[\frac{u_k^\epsilon(t_p+\epsilon)-u_k^\epsilon(t_p)}{\epsilon}\Big]\Big\}.\end{aligned}$$

According to Schwartz' distribution theory (Schwartz, 1966, 1983), both the convergence of the continuous functions $u_k^\epsilon(t)$ and $\dot{u}_k^\epsilon(t)$ towards their respective continuous limit $u_k(t)$ and piecewise-continuous limit $\dot{u}_k(t)$ justifies then the simplified final (and regular distribution) expressions for the work $\mathcal{P}_g[\boldsymbol{f},\boldsymbol{u}](t)$ in (C.9) with

$$\mathcal{P}_g[\boldsymbol{f}^i,\boldsymbol{u}](t) = \sum_{(k,t_p)\in\mathcal{N}\times\mathcal{T}_l[f_k](t)}\bar{p}_k(t_p)\mathrm{H}(t-t_p)\,\dot{u}_k(t_p^+) \tag{C.10a}$$

$$\mathcal{P}_g[\boldsymbol{f}^r,\boldsymbol{u}](t) \equiv \int_0^t\sum_{k\in\mathcal{N}} a\tilde{f}_k(\check{t})\,\dot{u}_k(\check{t})\,d\check{t} \equiv \mathcal{P}_r[\boldsymbol{f}^r,\boldsymbol{u}](t). \tag{C.10b}$$

To conclude let us also mentioned that one can obtain the same result with the interpolating TN PC solution proposed in Subsection 3.2 with Dirac's interpolation kernels.

References

Adelman, S.A., Doll, J.D., 1974. Generalized Langevin equation approach for atom/solid-surface scattering: collinear atom/harmonic chain model. J. Chem. Phys. 61 (10), 4242–4245. Erratum: Generalized langevin equation approach for atom/solid-surface scattering: Collinear atom/harmonic chain model. J. Chem. Phys. 62, 2518–2518 (1975)

Adelman, S.A., Doll, J.D., 1976. Generalized Langevin equation approach for atom/solid-surface scattering: general formulation for classical scattering off harmonic solids. J. Chem. Phys. 64 (4), 2375–2388.

Admal, N.C., Tadmor, E.B., 2010. A unified interpretation of stress in molecular systems. J. Elast. 100 (1–2), 63–143.

Admal, N.C., Tadmor, E.B., 2016. Material fields in atomistics as pull-backs of spatial distributions. J. Mech. Phys. Solids 89, 59–76.

Askes, H., Metrikine, A.V., Pichugin, A.V., Bennett, T., 2008. Four simplified gradient elasticity models for the simulation of dispersive wave propagation. Philos. Mag. 88 (28–29), 3415–3443.

Bishop, R.E.D., 1952. Longitudinal waves in beams. Aeronaut. Q. 3 (2), 280–293.

Blanc, X., Le Bris, C., Lions, P.-L., 2002. From molecular models to continuum mechanics. Arch. Ration. Mech. Anal. 164, 341–381.

Brillouin, L., Parodi, M., 1956. Propagation des ondes dans les milieux periodiques. Masson, Dunod, Paris.

Charlotte, M., 2001. Modèles discrets de rupture (Discrete Models of Fracture). PhD thesis of the university Pierre et Marie Curie (Paris 6).

Charlotte, M., Truskinovsky, L., 2002. Linear chain with a hyper-pre-stress. J. Mech. Phys. Solids 50, 217–251.

Charlotte, M., Truskinovsky, L., 2008. Towards multi-scale continuum elasticity theory. Continuum Mech. Thermodyn. 20, 133–161.

Charlotte, M., Truskinovsky, L., 2012. Lattice dynamics from a continuum viewpoint. J. Mech. Phys. Solids 60, 1508–1544.

Cheung, K.S., Yip, S., 1991. Atomic-level stress in an inhomogeneous system. J. Appl. Phys. 70 (10), 5688–5690.

Clausius, R.J.E., 1870. On a mechanical theorem applicable to heat. Philos. Mag. 40, 122–127.

Coleman, B.D., 1964a. On thermodynamics, strain impulses and viscoelasticity. Arch. Ration. Mech. Anal. 17, 230–254.

Coleman, B.D., 1964b. Thermodynamics of materials with memory. Arch. Ration. Mech. Anal. 17, 1–46.

Cosserat, E., Cosserat, F., 1909. Théorie de corps deformable. Hermann, Paris.

Eringen, A.C., 1966. Linear theory of micropolar elasticity. J. Math. Mech. 2, 909–924.

Eringen, A.C., 1972. Linear theory of nonlocal elasticity and dispersion of plane waves. Int. J. Eng. Sci. 10, 425–435.

Eringen, A.C., 1982. Nonlocal Continuum Field Theories. Springer-Verlag, New York.

Eringen, A.C., 1976. Nonlocal field theories. In: Eringen, A.C. (Ed.), Continuum Physics, 4, pp. 205–267. Academic press, New York

Eringen, A.C., Kim, B.S., 1977. Relation between non-local elasticity and lattice dynamics. Crystal Lattice Defects 7, 51–57.

Eringen, A.C., 1968. Theory of micropolar elasticity. In: Liebowitz, H. (Ed.), Fracture, 2, pp. 622–759. Academic press, New York

Español, P., 1996. Dissipative particle dynamics for a harmonic chain: a first principles derivation. Phys. Rev. E 53 (2), 1572–1578.

Fafalis, D.A., Filopoulos, S.P., Tsamasphyros, G.J., 2012. On the capability of generalized continuum theories to capture dispersion characteristics at the atomic scale. Eur. J. Mech. - A/Solids 36, 25–37.

Gibbs, J.W., 1928. On the equilibrium of heterogeneous substances collected works Longmans. In: Thermodynamics, Chap.III, I, p. 219. New-Yorks

Green, A.E., Naghdi, P.M., 1991. A re-examination of the basic postulates of thermomechanics. Proc. Math. Phys. Sci. 432 (1885), 171–194.

Green, A.E., Naghdi, P.M., 1993. Thermoelasticity without energy dissipation. J. Elast. 31, 189–208.

Hardy, R.J., 1982. Formulas for determining local properties in molecular dynamics simulation: shock waves. J. Chem. Phys. 76 (01), 622–628.

Il'iushina, E.A., 1969. On a model of continuous medium, taking into account the microstructure. Prikl. Matem. Mekhan. 33 (5), 917–923.

Irving, J.H., Kirkwood, G., 1950. The statistical mechanics theory of transport processes. iv. the equations of hydrodynamics. J. Chem. Phys. 18 (06), 817–829.

Jirásek, M., 2004. Nonlocal theories in continuum mechanics. Acta Polytechnica 44 (5–6).

Karpov, E.G., Park, H.S., Liu, W.K., 2007. A phonon heat bath approach for the atomistic and multiscale simulation of solids. Int. J. Numer. Methods Eng. 70, 351–378.

Kroner, E. (Ed.), 1968. Mechanics of generalized continua. Proceedings of IUTAM-Symposium. Springer, Berlin. ISBN 978-3-662-30259-0. doi:10.1007/978-3-662-30257-6.

Krumshansl, J.A., 1965. Generalized continuum field representation for lattice vibrations. In: Wallis, R.F. (Ed.), Lattice Dynamics, pp. 627–634. Pergamon, London

Kunin, I., 1982. Elastic Media with Microstructure, V.I (One Dimensional Models). Springer, Berlin.

Lagrange, J.-L., 1853. Mecanique analytique. Tome I, Second part, Section 6, 3rd edition. (In French)

Lehoucq, R.B., Lilienfeld-Toal, A., 2010. Translation of Walter Noll's "derivation of the fundamental equations of continuum thermodynamics from statistical mechanics". J. Elast. 100 (1–2), 5–24.

Lehoucq, R.B., Silling, S.A., 2008. Force flux and the peridynamic stress tensor. J. Mech. Phys. Solids 56, 1566–1577.

Love, A.E.H., 1927. A Treatise on the Mathematical Theory of Elasticity, 4th ed. Cambridge, p. pages173.

Love, A.E.H., 2009. A Treatise on the Mathematical Theory of Elasticity. Bibliolife, 2nd (1906) ed.

Maradudin, A.A., Montroll, E.W., Weiss, G.H., Ipatova, I.P., 1971. Theory of Lattice Dynamics in the Harmonic Approximation. Academic Press, New-York.

Mauricio, F., Velasco, S., 1984. Use of the memory function in a collinear atom/harmonic chain model. J. Chem. Phys. 81 (4), 2064–2069.

Maxwell, J.C., 1870. On reciprocal figures, frames and diagrams of forces. Trans. R. Soc. Edinborough XXVI 1–43.

Maxwell, J.C., 1874. Van der waals: on the continuity of the gaseous and liquid states. Nature 477–480.

Metrikine, A., Askes, H., 2002a. One-dimensional dynamically consistent gradient elasticity models derived from a discrete microstructure. part1: generic formulation. Eur. J. Mech. A/ Solids 21, 555–572.

Metrikine, A., Askes, H., 2002b. One-dimensional dynamically consistent gradient elasticity models derived from a discrete microstructure. part2: static and dynamic response. Eur. J. Mech. A/ Solids 21, 573–588.

Milton, G.W., Willis, J.R., 2007. On modifications of Newton's second law and linear continuum elastodynamics. Proc. R. Soc. London A 463, 855–880.

Mindlin, R., 1964. Micro-structure in linear elasticity. Arch. Ration. Mech. Anal. 10, 51–77.

Mindlin, R., 1965. Second gradient of strain and surface tension in linear elasticity. Int. J. Solids Struct. 1, 417–438.

Mindlin, R., Herrmann, G., 1950. A one-dimensional theory of compressional waves in an elastic rod. In: Proceedings of the First U.S. National Congress of Applied Mechanics, pp. 187–191.

Mindlin, R., McNiven, H., 1960. Axially symmetric waves in elastic rods. Trans. ASME, J. Appl. Mech. 145–151.

Mori, H., 1965. Transport, collective motion, and Brownian motion. Prog. Theor. Phys. 33 (3), 423–455.

Mühlhaus, H.-B., Oka, F., 1996. Dispersion and wave propagation in discrete and continuous models for granular materials. Int. J. Solids Struct. 33, 2841–2858.

Murdoch, A.I., 1982. The motivation of continuum concepts and relations from discrete considerations. J. Appl. Math. Mech. 36, 163–187.

Murdoch, A.I., 2003. On the microscopic interpretation of stress and couple stress. J. Elast. 71, 105–131.

Murdoch, A.I., 2007. A critique of atomistic definitions of the stress tensor. J. Elast. 88, 113–140.

Murdoch, A.I., Bedeaux, D., 1993. On the physical interpretation of fields in continuum mechanics. Int. J. Eng. Sci. 31 (10), 1345–1373.

Murdoch, A.I., Bedeaux, D., 1994. Continuum equations of balance via weighted averages of microscopic quantities. Proc. R. Soc. London A 445, 157–179.

Myshkis, A.D., Filimonov, A.M., 2003. About the string with beads. Matematicheskaya fizika, analiz, geometriya 10 (3), 301–306.

Noll, W., 1955. Die herleitung der grundgleichungen der thermomechanik der kontinua aus der statistischen mechanik. J. Ration. Mech. Anal. 4, 627–646. An english translation was provided by Ref. (Lehoucq and Lilienfeld-Toal, 2010)

Noll, W., 2009. Thoughts on the concept of stress. Department of Mathematical Sciences, Paper 18. Published on the website http://repository.cmu.edu/math/18

Park, H.S., Karpov, E.G., Liu, W.K., Klein, P.A., 2005. The bridging scale for two-dimensional atomistic/continuum coupling. Philos. Mag. 85 (1), 79–113.

Park, H.S., Liu, W.K., 2004. An introduction and tutorial on multi-scale analysis in solids. Comput. Methods Appl. Mech. Eng. 193, 1733–1772.

Petrov, Y.V., Gruzdkov, A.A., Kazarinov, N.A., 2008. Features of the dynamic fracture of one-dimensional linear chains. Doklady Phys. 53 (11), 595–599.

Pichugin, A.V., Askes, H., Tyas, A., 2008. Asymptotic equivalence of homogenisation procedures and fine-tuning of continuum theories. J. Sound Vib. 313, 858–874.

Rayleigh, J.W., 1945. Theory of Sound, vol. I. Dover Publications, New York.

Roddier, F., 1971. Distributions et transformation de fourier. In: Ediscience, pp. 57–64. Paris, chap. 4.

Rogula, D., 1982. Introduction to nonlocal theory of material media in: nonlocal theory of elastic media. In: CISM Courses, 268, pp. 123–222. Springer, Berlin.

Schwartz, L., 1966. Théorie des distributions. Hermann, Paris.

Schwartz, L., 1983. Méthodes mathématiques pour les sciences physiques. Hermann, Paris.

Shenoy, V.B., Miller, R., Tadmor, E.B., Rodney, D., Phillips, R., Ortiz, M., 1999. An adaptive methodology for atomic scale mechanics: the quasicontinuum method. J. Mech. Phys. Solids 47, 611–642.

Silling, S.A., 2000. Reformulation of elasticity theory for discontinuities and long-range forces. J. Mech. Phys. Solids 48, 175–209.

Slepyan, L. I., 1972. Non-stationary Elastic Waves. Sudostroenie, Leningrad (in Russian) (1972).

Slepyan, L.I., 2002. Models and Phenomena in Fracture Mechanics. Springer, Berlin, p. page576.

Suiker, A.S.J., de Borst, R., 2005. Enhanced continua and discrete lattices for modelling granular assemblies. Philos. Trans. R. Soc. A 363, 2543–2580.

Suiker, A.S.J., Metrikine, A.V., de Borst, R., 2001. Comparison of wave propagation characteristics of the Cosserat continuum model and corresponding discrete lattice models. Int. J. Solids Struct. 38, 1563–1583.

Sunyk, R., Steinmann, P., 2003. On higher gradients in continuum-atomistic modelling. Int. J. Solids Struct. 40, 6877–6896.

Tadmor, E.B., Miller, R.E., 2011. Modeling Materials: Continuum, Atomistic and Multiscale Techniques. Cambridge University Press.

Tadmor, E.B., Ortiz, M., Philips, R., 1996. Quasicontinuum analysis of defects in solids. Philos. Mag. A 73, 1529–1563.

Tadmor, X.L., E., W., 2007. Variational boundary conditions for molecular dynamics simulations of crystalline solids at finite temperature: treatment of the thermal bath. Phys.rev. B 76, 104107.

Tadmor, X.L., E., W., 2008. Variational boundary conditions for molecular dynamics simulations: Treatment of the loading condition. J. Comp. Phys 227, 10078–10093.

Tang, S., Hou, T.Y., Liu, W.K., 2006. A mathematical framework of the bridging scale method. Int. J. Numer. Methods Eng. 65, 1688–1713.

Timoshenko, S.P., 1983. History of Strength of Materials. Dover, pp. pages108–109. Unabridged and unaltered republication of the 1953 book originally published by McGraw-Hill Book Company, Inc., N.Y.

Toupin, R.A., 1962. Elastic materials with couple stresses. Arch. Ration. Mech. Anal. 11, 385–414.

Tsai, D.H., 1979. The virial theorem and stress calculation in molecular dynamics. J. Chem. Phys. 70 (03), 1375–1382.

Vasiliev, A.A., Dmitriev, S.V., Bishop, A.R., Miroshnichenko, A.E., 2010. Multi-field approach in mechanics of structural solids. Int. J. Solids Struct. 47 (3–4), 510–525.

Willis, J.R., 1981. Variational and related methods for the overall properties of composites. Adv. Appl. Mech. 21, 1–78.

Willis, J.R., 1997. Dynamics of composites. In: Suquet, P. (Ed.), Continuum Micromechanics: CISM Courses and Lectures, 377. Springer-Verlag-Wien, New York, pp. 265–290.

Wolf, K.B., 1979. Integral Transforms in Science and Engineering. Plenum Press, New-York.

Zhou, M., 2003. A new look at the atomic level virial stress: on continuum-molecular system equivalence. Proc. R. Soc. London A 459, 2347–2392.

Zimmerman, J.A., Jones, R.E., Klein, P.A., Bammann, D.J., Webb III, E.B., Hoyt, J.J., 2002. Continuum Definitions for Stress in Atomistic Simulation. Sand report, SAND2002-8608, chap. 4.

Zimmerman, J.A., Jones, R.E., Templeton, J.A., 2010. A material frame approach for evaluating continuum variables in atomistic simulations. J. Comput. Phys. 229, 2364–2389.

Zimmerman, J.A., Webb III, E.B., Hoyt, J.J., Jones, R.E., Klein, P.A., Bammann, D.J., 2004. Calculation of stress in atomistic simulation. Model. Simul. Mater. Sci. Eng. 12, S319–S332.

Zwanzig, R.W., 1960. Collision of a gas atom with a cold surface. J. Chem. Phys. 32, 1173.